through a column (RNeasy mini kit; Qiagen) and dissolved in RNase-free water. The concentration was determined by measuring the optical density at 260 nm, and RNA integrity was checked by nondenaturing agarose gel electrophoresis.

RNA transfection and selection of G418-resistant cells. Subconfluent Huh-7 cells were trypsinized, washed once with phosphate-buffered saline (PBS) (−), and resuspended at 10^7 cells/ml in OPTI-MEM (Gibco-BRL, Invitrogen Life Technologies). Then, 10 to 1,000 ng of transcript was adjusted with total RNA from naive Huh-7 cells to a final amount of 10 μg, which was mixed with 400 μl of the cell suspension in a cuvette with a gap width of 0.4 cm (Bio-Rad). The mixture was immediately transfected into Huh-7 cells by electroporation with GenePulser II system (Bio-Rad) set to 270 V and 975 μF. Following 10 min of incubation at room temperature, the cells were transferred into 10 ml of growth medium and then seeded into a 10- or 15-cm-diameter cell culture dish. For the selection of G418-resistant cells, the medium was replaced with fresh medium containing 0.5 to 1 mg of G418 (Geneticin; Gibco-BRL, Invitrogen Life Technologies)/ml after 24 to 48 h and the medium was changed twice a week. Four weeks after transfection, colonies were stained with Coomassie brilliant blue (0.6 g/liter in 50% methanol–10% acetic acid).

IFN treatment. To stop the replication of HCV subgenomic RNA, 50-1 cells were treated with 10,000 U of IFN-α2b (kindly provided by Schering-Plough)/ml in the absence of G418. After 2 weeks of IFN treatment, the absence of HCV RNA was determined from the results of Northern hybridization, reverse transcription-PCR, and sensitivity to G418.

Cell culture. We used two kinds of Huh-7 cells, one derived from our own laboratory's original Huh-7 cell line, designated Huh-7-DMB, and the cured clone of 50-1 cells, designated Huh-7-KV-C. Both types of Huh-7 cells were grown in Dulbecco's modified Eagle's medium (Gibco-BRL, Invitrogen Life Technologies) supplemented with 10% fetal bovine serum, 2 mM L-glutamine, nonessential amino acids, 100 U of penicillin, and 100 μg of streptomycin.

Preparation of cell extracts, coprecipitation with glutathione resin, and Western blot analysis. The transient transfection of COS1 cells was carried out by using the calcium-phosphate method. The cells were harvested, washed with PBS (−), and sonicated in PBS lysis buffer [PBS (−) containing 250 mM NaCl, 1.0% Triton X-100, 1 mM EDTA, and 1 mM dithiothreitol] with 10 mg (each) of aprotinin and leupeptin per ml. Total cell lysate was diluted 10-fold with PBS lysis buffer, mixed with 40 μl of glutathione-Sepharose 4B beads (glutathione resin) (Amersham Biosciences), and then incubated for 3 h on a rotator in a cold room. After an extensive wash with PBS (−) containing 1.0% Triton X-100, the bound proteins were eluted, fractionated by sodium dodecyl sulfate (SDS)–10% polyacrylamide gel electrophoresis (PAGE), transferred onto nitrocellulose membranes, and subjected to Western blot analysis with anti-FLAG monoclonal antibody. The proteins were visualized by enhanced chemiluminescence according to the manufacturer's instructions (Amersham Biosciences). The nitrocellulose membranes used for Western blot analysis with anti-FLAG monoclonal antibody were reprobed with anti-GST monoclonal antibody (Zymed Laboratories) according to the manufacturer's instructions (Amersham Biosciences).

RESULTS

Interaction between NS5A and NS5B. It was previously reported that NS5A and NS5B associate through two discontinuous regions of NS5A (aa 105 to 162 and 277 to 334) and that NS5A weakly stimulates the activity of NS5B RdRp in vitro initially (at a molar ratio to NS5B of less than 0.1) and then inhibits the activity in a dose-dependent manner (54). To examine the effect of this interaction on HCV RNA replication, we used an HCV RNA replicon system derived from the isolate M1LE and 50-1 cells (33). We prepared a hybrid replicon of JK-1 and M1LE which harbors the JK-1 sequence from aa 92 (*Mlu*I site) of NS5A to the end of NS5B. However, the hybrid replicon did not produce any G418-resistant colony with the Huh-7 cell line (data not shown), so we constructed various mutated versions of NS5A of the RNA replicon derived from M1LE.

First, we confirmed whether the association between NS5A and NS5B through the two discontinuous regions of NS5A occurs with the sequence derived from M1LE. COS1 cells were transiently cotransfected with mammalian expression vectors, pNKFLAG-5A/wild, /del-1, /del-2, and /del-3; pNKGST or pNKGST-5B/wild; and the cell lysates were subjected to a GST pull-down assay. pNKFLAG-5A/wild encodes the full-length and wild-type NS5A proteins of M1LE. pNKFLAG-5A/del-1 encodes the internally deleted NS5A protein missing aa 94 to 162, a deletion 11 aa longer than that reported for JK-1 for the convenience of mutagenesis (aa 105 to 162). pNKFLAG-5A/del-2 encodes the internally deleted NS5A protein missing aa 277 to 334, the same region reported for JK-1. pNKFLAG-5A/del-3 encodes the internally deleted NS5A protein missing aa 235 to 276, a region nonessential for the interaction with NS5B in JK-1. pNKGST-5B/wild encodes the full-length and wild-type NS5B proteins of M1LE, and pNKGST encodes only a GST protein. Under conditions in which the expression levels of FLAG-NS5A proteins (input) were similar and the recovery of the GST-NS5B proteins was almost the same (Fig. 1A, lanes 1 to 5, and C, lanes 2 to 5), coprecipitated NS5A proteins (output) were examined (Fig. 1B, lanes 1 to 5). FLAG-NS5A/wild bound to GST-NS5B (Fig. 1B, lane 2) but not to GST alone (Fig. 1B, lane 1). This result demonstrates that NS5A and NS5B also interact not only in JK-1 but also in M1LE in vivo. Very little FLAG-NS5A/del-1 or /del-2 was recovered (Fig. 1B, lane 3 and 4); however, FLAG-NS5A/del-3 was efficiently pulled down (Fig. 1B, lane 5). When larger amounts of proteins were used for this assay, both FLAG-NS5A/del-1 and /del-2 were weakly detected in the fraction pulled down with GST-NS5B but much significantly weaker than FLAG-5A/wild and /del-3. These results demonstrate that aa 94 to 162 (defined as region 1) and aa 277 to 334 (region 2), but not aa 235 to 276 (region 3), of NS5A seem to be essential for binding NS5B in M1LE as observed in JK-1.

Effect of binding NS5B on HCV RNA replication. To examine the effect of the interaction between NS5A and NS5B on HCV RNA replication in the replicon system, we prepared three kinds of internal deletion mutants, M1LE/5Adel-1, M1LE/5Adel-2, and M1LE/5Adel-3, missing regions 1, 2, and 3 of NS5A, respectively (Fig. 2). M1LE/5Adel-1 and M1LE/5Adel-2 are impaired in their binding to NS5B, but M1LE/5Adel-3 is not. As a negative control, we prepared M1LE/5B-VDD, in which the GDD motif of NS5B was mutated to VDD.

FLAG-tagged wild-type and internally deleted NS5A proteins were efficiently expressed in transiently transfected COS1 cells (Fig. 3). When wild-type M1LE and M1LE/5Adel-3 were transfected by electroporation into our laboratory's Huh-7 cell line, Huh-7-DMB, G418-resistant colonies emerged after selection at a concentration of 1 mg/ml. In the case of M1LE/5Adel-3, the number of G418-resistant colonies was about seven times fewer than in wild-type M1LE. In contrast, no colonies emerged when M1LE/5Adel-1, M1LE/5Adel-2, and M1LE/5B-VDD were transfected into Huh-7-DMB cells, indicating that both of the NS5B-interacting regions of NS5A are critical for HCV RNA replication (Fig. 4). The fact that M1LE/5Adel-3 was replication competent but less efficient than the wild type in Huh-7-DMB cells may reflect some roles of region 3 in HCV RNA replication or a conformational change introduced by the internal deletion (see Discussion).

To minimize the effect of the internal deletion and further delineate the sequence(s) critical for HCV RNA replication, we used the alanine-scanning method (7). All residues of the two regions were scanned by introducing alanine substitution

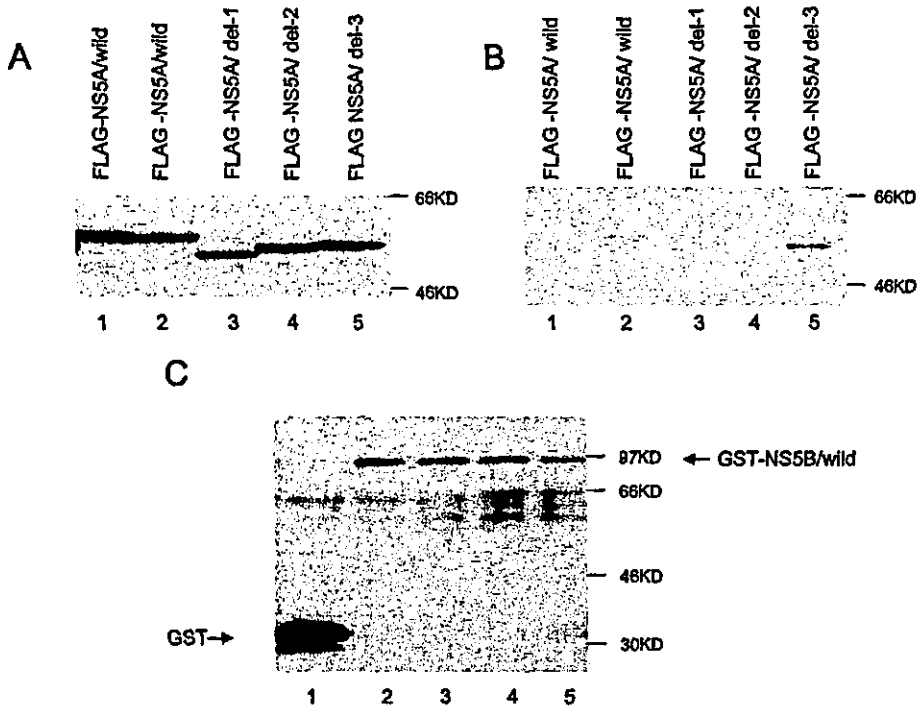

FIG. 1. Interaction between NS5A and NS5B of the isolate HCV M1LE and the regions essential for this interaction. COS1 cells were transiently cotransfected with mammalian expression vectors expressing FLAG-NS5A proteins (lanes: 1 and 2, wild type; 3, internal deletion mutant 1; 4, internal deletion mutant 2; 5, internal deletion mutant 3) and GST protein alone (lane 1) or GST-NS5B proteins (lanes 2, 3, 4, and 5). (A) Input of FLAG-NS5A proteins. Total lysates were fractionated by SDS–10% PAGE and subjected to Western blot analysis with anti-FLAG monoclonal antibody. (B) Output of FLAG-NS5A proteins. Coprecipitants by glutathione resin were washed with PBS (−) containing 1.0% Triton X-100, fractionated by SDS–10% PAGE, and subjected to Western blot analysis with anti-FLAG monoclonal antibody. (C) Recovery of GST or GST-NS5B proteins. The nitrocellulose membrane used for Western blot analysis of coprecipitants with anti-FLAG antibody was reprobed with anti-GST antibody. Molecular masses (in kilodaltons) are indicated to the right of each panel.

cm in addition to one cm mutant within region 3 as a control (Fig. 2). All of these cm mutants in FLAG-tagged forms, 10 in region 1, 9 in region 2, and 1 in region 3, were similarly expressed in transiently transfected COS1 cells (Fig. 3). When these 20 mutants were transfected by electroporation into Huh-7-DMB cells, only M1LE/cm 252, 277, 283, 290, 297, and 304 were found to be replication competent, although less so than wild-type M1LE. All other mutants were replication incompetent (Fig. 5). The regions of cm 252, 277, 283, 290, 297, and 304 are predicted to form a helical structure by DNASIS-Mac, version 3.2 (Hitachi Software Engineering Co.). The competence of replication may be due to this original structure (see Discussion). To rule out this possibility, we constructed another cm mutant, M1LE/cm 110. In this mutant, the region from aa 110 to 117 of NS5A is predicted to form a helical structure, were all changed to alanines, and after the transfection into Huh-7-DMB cells, no colonies emerged (data not shown). These results support the notion that the inability of the internal deletion mutants, M1LE/5Adel-1 and M1LE/5Adel-2, to replicate is due not to conformational change induced by the deletions but to the absence of interaction between NS5A and NS5B. It is also unlikely that these results are due to an increased cytotoxicity associated with the mutant NS5As, because we observed no decrease in transfection efficiency or ability to establish colonies by using the plasmid encoding a drug resistance marker along with the wild or the mutant NS5A protein (data not shown).

Improvement in the HCV replicon system. The results clearly showed that two discontinuous regions of NS5A are essential for HCV RNA replication by using the HCV replicon system with Huh-7-DMB cells; however, the number of G418-resistant colonies per microgram of transfected RNA was much smaller than previously reported (24, 29, 35, 37). It remains unclear whether some mutants were replication competent but too inefficient to be detected in the system we applied. Therefore, we tried to improve the assay system in two ways, by the introduction of point mutations to NS5A and by the selection of Huh-7 cells cured of HCV RNA replication by IFN treatment.

We constructed three mutants, M1LE/S225P, M1LE/delS229, and M1LE/S232I, harboring the point mutation S225P (35), a deletion of S229 (delS229) (24), and S232I (4), respectively, all defined as adaptive mutations in other HCV replicon systems (Fig. 2). Next, the 50-1 cells, an HCV subgenome-replicating subclone, were cured of HCV RNA by treatment with IFN for 2 weeks (as described in Materials and Methods), and then the absence of HCV RNA was determined from the results of Northern hybridization, reverse transcription-PCR, and sensitivity to G418 (data not shown). The 50-1 cells cured of HCV RNA by treatment with IFN, designated

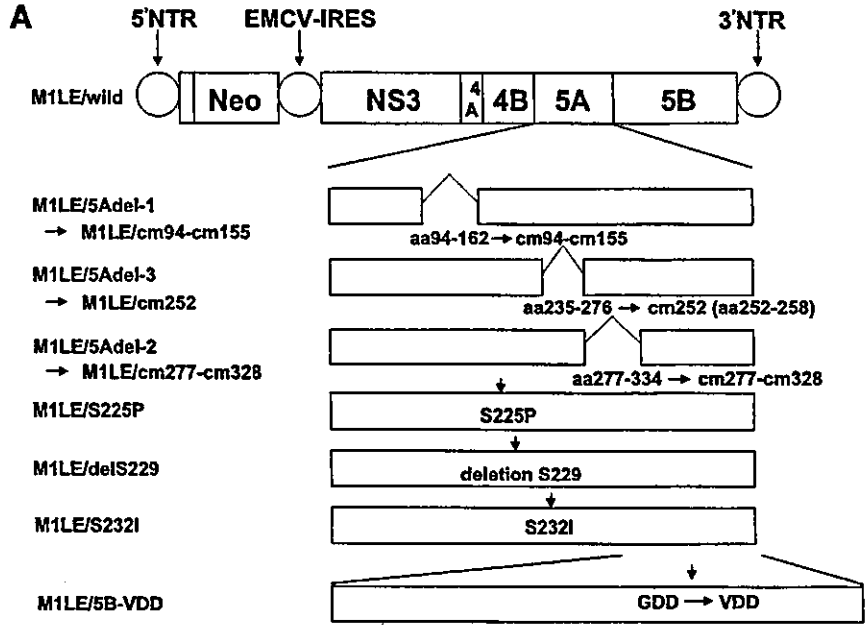

FIG. 2. (A) Schematic presentation of HCV mutant replicons used in this study. Wild-type M1LE contains the HCV M1LE wild-type sequence. M1LE/5Adel-1, M1LE/5Adel-2, and M1LE/5Adel-3 encode internal deletions of NS5A missing aa 94 to 162 (region 1), aa 277 to 334 (region 2), and aa 235 to 276 (region 3), respectively. All amino acids within region 1 were replaced with alanines, and 11 cm mutants were prepared. All amino acids within region 2 were replaced, and 9 cm mutants were prepared. The aa 252 to 258 within region 3 were replaced, and M1LE/cm 252 was prepared. The point mutation S225P, a deletion of S229, and S232I were introduced into wild-type M1LE, and then M1LE/S225P, M1LE/delS229, and M1LE/S232I were prepared. M1LE/5B-VDD encodes NS5B in which the GDD motif was mutated to VDD. (B) Summary of the NS5A mutations. This figure shows the entire amino acid sequence of NS5A of M1LE and the positions of mutations. Numbering starts from the beginning of NS5A. Internal deletions 1, 2, and 3, and point mutations S225P, delS229, and S232I, and cm 252 were introduced as described for panel A. All amino acids within region 1 were replaced with alanines, and then M1LE/cm 94, 100, 105, 110, 113, 120, 127, 134, 141, 148, and 155 were prepared. All amino acids within region 2 were replaced with alanines, and M1LE/cm 277, 283, 290, 297, 304, 311, 316, 321, and 328 were prepared. The positions of the substituted amino acids in each cm mutant are shown in panel B.

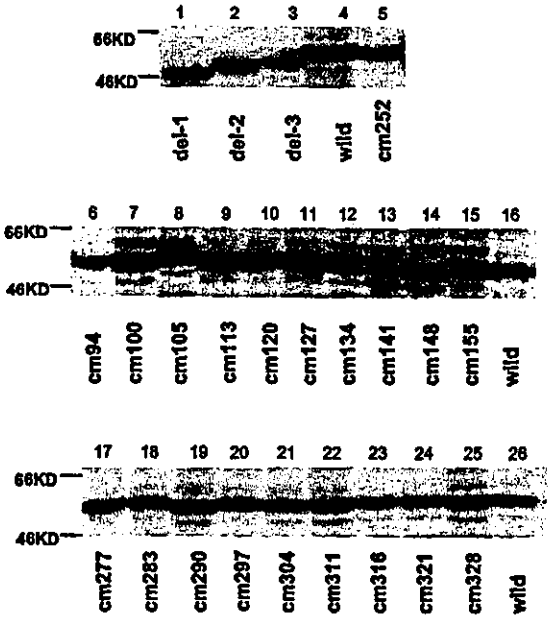

FIG. 3. Efficient translation of mutant FLAG-NS5As. COS1 cells were transiently transfected with mammalian expression vectors expressing FLAG-NS5A proteins that were prepared as described in Materials and Methods. Lanes: 4, 16, and 26, wild type; 1, internal deletion 1; 2, internal deletion 2; 3, internal deletion 3; 5, cm 252; 6, cm 94; 7, cm 100; 8, cm 105; 9, cm 113; 10, cm 120; 11, cm 127; 12, cm 134; 13, cm 141; 14, cm 148; 15, cm 155; 17, cm 277; 18, cm 283; 19, cm 290; 20, cm 297; 21, cm 304; 22, cm 311; 23, cm 315; 24, cm 321; 25, cm 328. Total lysates were fractionated by SDS–10% PAGE and subjected to Western blot analysis with anti-FLAG monoclonal antibody. Molecular masses (in kilodaltons) are indicated to the left of the panels.

Huh-7-KV-C, were evaluated. Wild-type and these mutant HCV replicons were transfected into Huh-7-DMB and Huh-7-KV-C cells. In Huh-7-DMB cells, M1LE/S225P and M1LE/S232I actually increased the efficiency of transduction to some extent, but M1LE/delS229 did not (Fig. 6A). M1LE/S232I was the most effective. In Huh-7-KV-C cells, interestingly, no colonies emerged after selection with G418 when wild-type M1LE was transfected, whereas in the case of M1LE/S225P, delS229, and S232I, 2,500, 3,000, and 25,000 colonies/μg of RNA emerged, respectively (Fig. 6B). These results indicate that two point mutations, S225P and S232I, can be categorized as the adaptive mutations in the isolate M1LE and that the cells cured of HCV RNA by treatment with IFN, Huh-7-KV-C, show higher permissiveness for M1LE/S225P, delS229, and S232I than Huh-7-DMB cells. In this way, we established highly improved replicon systems.

Delineation of important sequences of NS5A for HCV RNA replication. To examine the effect of internal deletions and alanine substitutions on HCV RNA replication with this improved replicon system, double mutants with S232I plus internal deletion mutations or alanine-substituted cm's in M1LE were constructed and transfected into Huh-7-DMB and Huh-7-KV-C cells by electroporation. After G418 selection, in Huh-7-DMB cells, some 400 to 1,000 colonies/μg of RNA emerged with the double mutants of M1LE/S232I plus cm 252, 277, 283, 297, and 304, but only about 100 colonies/μg of RNA emerged with the double mutant M1LE/S232I plus cm 290. No colonies emerged with the double mutant M1LE/S232I plus other cm's, del-1, del-2, and del-3 (Fig. 7; data not shown for Huh-7-KV-C cells). The double mutant M1LE/S232I plus cm 110 was also replication incompetent in Huh-7-DMB cells. To further examine the replication competence of these mutants, double mutants of M1LE/S225P plus an internal deletion mutation or cm were constructed and then transfected into Huh-7-DMB cells. The results were almost the same as those with the double mutants with S232I, although the efficiencies of these mutants were around one-half of those with S232I (Fig. 8). The similar results in the double mutants with S225P were obtained with Huh-7 KV-C cells (data not shown). The replication-defective property of the mutants with deletions of regions 1 and 2, the cm mutants within region 1, and the cm mutants in the C-terminal part of region 2 was also observed with both Huh-7-DMB and Huh-7-KV-C cells, indicating that the replication incompetence of these mutants is not due to the low efficiency of the original assay system. The cm mutants at the N-terminal part of region 2, cm 277, 283, 290, 297, and 304, were replication competent in the absence of the adaptive mutation in Huh-7-DMB cells and also in the presence of the adaptive mutation in Huh-7-DMB and Huh-7-KV-C cells to some extent. Taken together, these results suggest that the interaction with NS5B through regions 1 and 2, probably through its C-terminal part, is also essential for HCV RNA replication. We examined the interaction between cm mutants of FLAG-NS5A and GST-NS5B, but the difference among wild-type and cm mutants was weak in the pull-down assay. Differential binding would be possible if the two partner proteins were lower in concentration or together with other NS proteins, as those occur in vivo in HCV-RNA-replicating cells.

Interestingly, two quantitative differences were observed with M1LE/5Adel-3, cm 252, and 290 with and without the adaptive mutations. M1LE/5Adel-3 was weakly replication competent in Huh-7-DMB cells but incompetent in Huh-7-DMB and Huh-7-KV-C cells when the adaptive mutations were introduced. In contrast, M1LE/cm 252 was weakly replication competent in Huh-7-DMB cells but as high as that of the other replication-competent cm mutants in the presence of the adaptive mutations in Huh-7-DMB and Huh-7-KV-C cells (data not shown for Huh-7-KV-C cells; see Discussion).

DISCUSSION

HCV NS5A is a viral regulatory protein that modulates viral RNA replication and host processes by interacting directly and indirectly with a variety of host regulatory factors (10, 19, 42, 56, 58, 67). The important role of NS5A in HCV RNA replication has been clearly demonstrated by high or clustered incidence of adaptive mutations in NS5A detected in HCV RNA replicon systems, although the molecular mechanism involved remains unknown (4, 24, 35, 37, 40). Shirota et al. previously reported direct interaction between NS5A and NS5B through two binding regions of NS5A expressed in mammalian cells and in vitro with a purified recombinant and that NS5A could modulate the activity of NS5B RdRp in vitro through this direct interaction (54). Here we demonstrated the critical role of regions essential for the NS5A-NS5B interaction in HCV RNA replication with an HCV subgenomic replicon by introducing several internal deletion mutations into

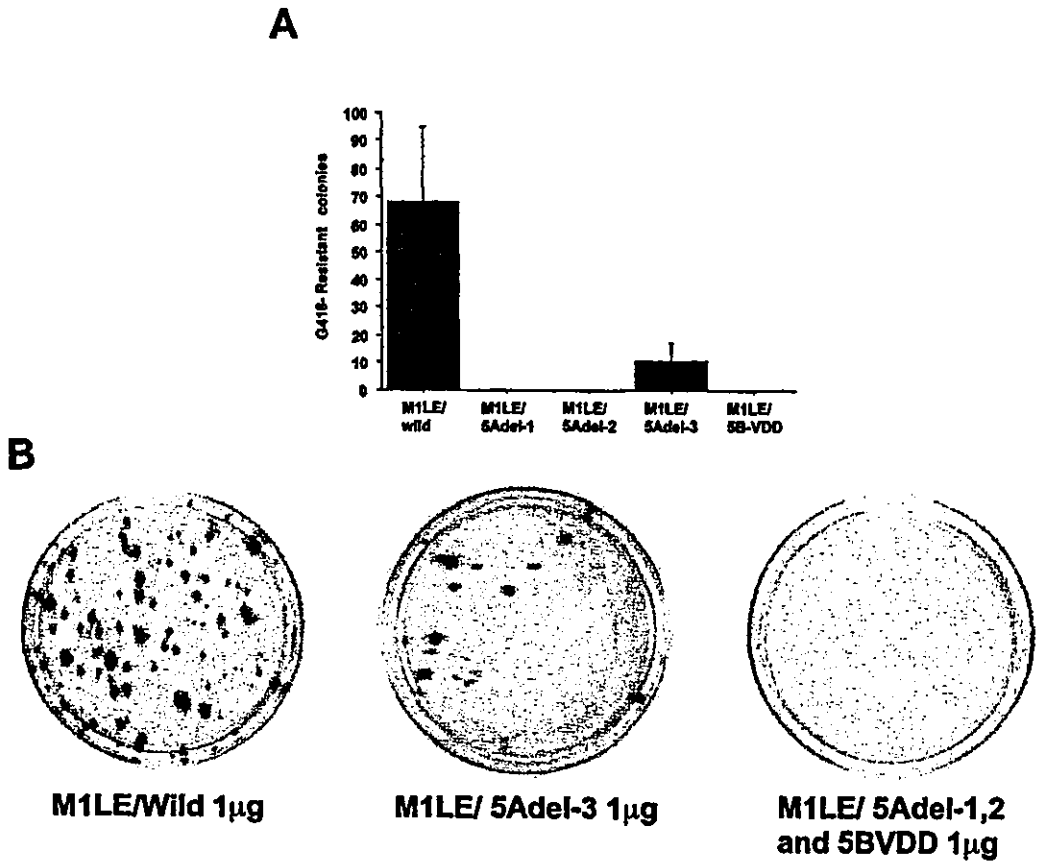

FIG. 4. Effect of internal deletion mutation on HCV RNA replication. Huh-7-DMB cells were transfected with 1 μg of in vitro-transcribed wild-type MILE, 5Adel-1, 5Adel-2, 5Adel-3, and 5B-VDD RNA by electroporation, and G418-resistant cells were selected with a G418 concentration of 1 mg/ml. G418-resistant cell colonies were stained 4 weeks after transfection. (A) This figure shows the mean number of G418-resistant cell colonies isolated per 10-cm-diameter cell culture dish per 1 μg of RNA. Error bars indicate the standard deviations of the results from at least three independent experiments. (B) G418-resistant colonies were visualized by staining cells as described in Materials and Methods.

NS5A. Our results provide clear evidence that NS5A is indispensable for HCV RNA replication probably through its interaction with NS5B, since the mutants missing the NS5B-binding regions, regions 1 and 2, could not produce G418-resistant colonies, but the mutants missing region 3, which is not essential for this interaction, could. The critical role of NS5A in HCV RNA replication in this report is consistent with the previous one that an amino-terminal amphipathic α-helix of NS5A is essential for HCV RNA replication in the replicon system, localizing NS5A to a membrane (13). The use of cm mutants strongly suggests that all of region 1 and the C-terminal part of region 2 are critical for HCV RNA replication. However, it is difficult to exclude the possibility that the substitution of eight amino acids in a row may induce structural change. Then the critical regions defined by cm mutants may simply reflect the structural integrity necessary for the function, although a structural evaluation is difficult at present, since no crystal model of NS5A is available. Further mutational analysis is necessary to test these possibilities.

HCV RNA replication would take place in a distinctly altered membrane structure of the endoplasmic reticulum, a membranous web (12), as recently reported by Gosert et al. (20). All NS proteins might be recruited to the membrane structure via their own membrane association domains or by the help of NS4A in the case of NS3 (8, 13, 20, 28, 30, 51, 52, 63). Recently, Dimitrova et al. (11) reported that all six NS proteins interact with each other through their multiple interacting surfaces. NS5B is HCV RdRp and has been reported to interact with NS proteins and some host proteins. Such interaction(s) may modulate the activity of NS5B RdRp in various ways. The critical role of the homomeric interaction of NS5B in RdRp activity was demonstrated by us and another group (48, 60). Piccininni et al. (47) reported that NS5B interacts with NS3 and NS4B as positive and negative regulators in the replication complex. Previously, it was reported that the direct binding of NS5A and NS5B in the isolate JK-1 weakly stimulated the activity of NS5B RdRp in vitro at first (at a molar ratio to NS5B of less than 0.1) and then inhibited the activity in a dose-dependent manner (54). In the present study, we showed that the two regions of NS5A are important for binding NS5B and are essential for HCV RNA replication in the isolate M1LE by HCV replicon assays. The weak stimulation by NS5A of RdRp activity through the binding of NS5B observed in vitro may reflect the essential role of NS5A in HCV RNA replication, or the interaction between NS5A and NS5B is important for the dynamic assembly of NS proteins in the HCV

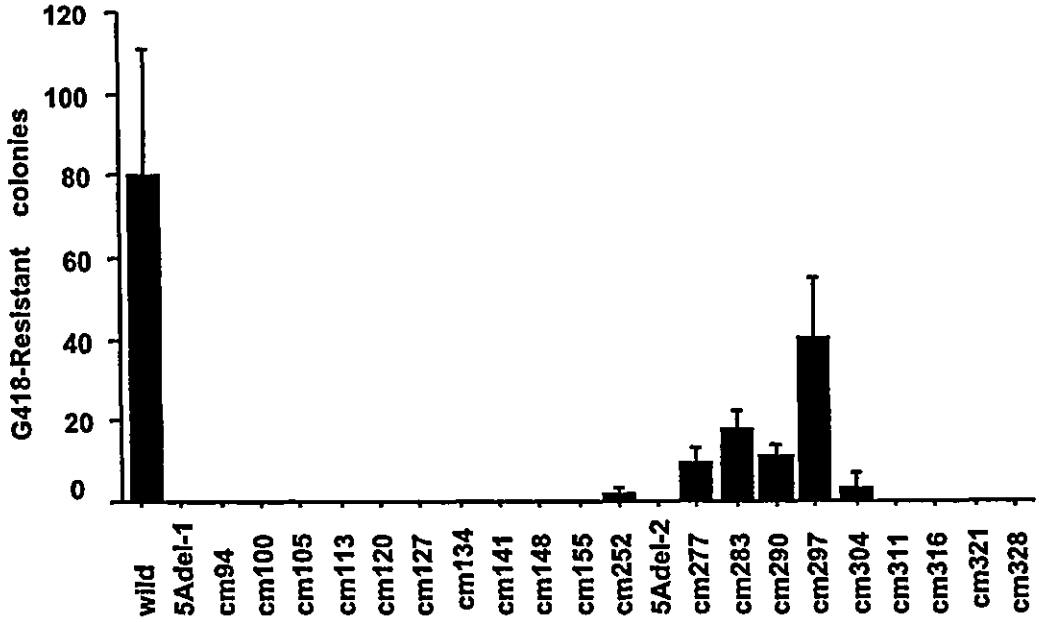

FIG. 5. Effect of clustered alanine-substitution mutations on HCV RNA replication. Huh-7-DMB cells were transfected with 1 μg of in vitro-transcribed wild-type M1LE, 5Adel-1, 5Adel-2, and cm 94, 100, 105, 113, 120, 127, 134, 141, 148, 155, 252, 277, 283, 290, 297, 304, 311, 316, 321, and 328 RNA, and G418-resistant cells were selected with a G418 concentration of 0.5 mg/ml. G418-resistant cell colonies were stained 4 weeks after transfection. This figure shows the mean number of G418-resistant cell colonies isolated per 15-cm-diameter cell culture dish per 1 μg of RNA. Error bars indicate the standard deviations of the results from at least three independent experiments.

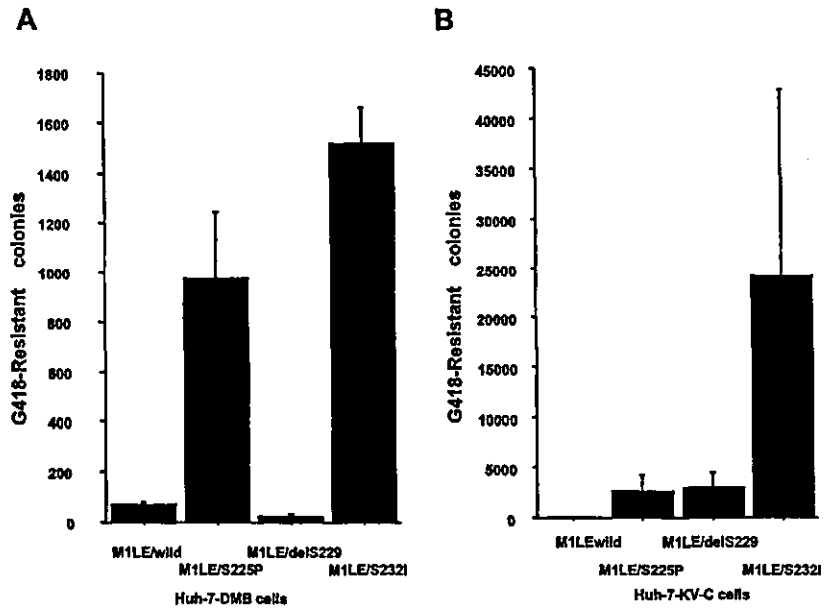

FIG. 6. Effects of three kinds of point mutation, S225P, deletion S229, and S232I, on HCV RNA replication in the Huh-7-DMB and KV-C sublines. 50-1 cells were cured of self-replicating subgenomic RNAs by IFN-α treatment, and then cured 50-1 cells, Huh-7-KV-C, were prepared. Huh-7-DMB and KV-C cells were transfected with 10 ng to 1 μg of in vitro-transcribed wild-type M1LE, M1LE/S225P, M1LE/delS229, and M1LE/S232I RNA. G418-resistant cells were selected with a G418 concentration of 1 mg/ml. G418-resistant cell colonies were stained 4 weeks after transfection. (A) This figure shows the mean number of G418-resistant cell colonies isolated per 10-cm-diameter cell culture dish per 1 μg of RNA when each in vitro-transcribed mutant RNA was transfected into Huh-7-DMB cells. Error bars indicate the standard deviations of the results from at least three independent experiments. (B) This figure shows the mean number of G418-resistant cell colonies isolated per 10-cm-diameter cell culture dish per 1 μg of RNA when each in vitro-transcribed mutant RNA was transfected into Huh-7-KV-C cells. Error bars indicate the standard deviations of the results from at least three independent experiments.

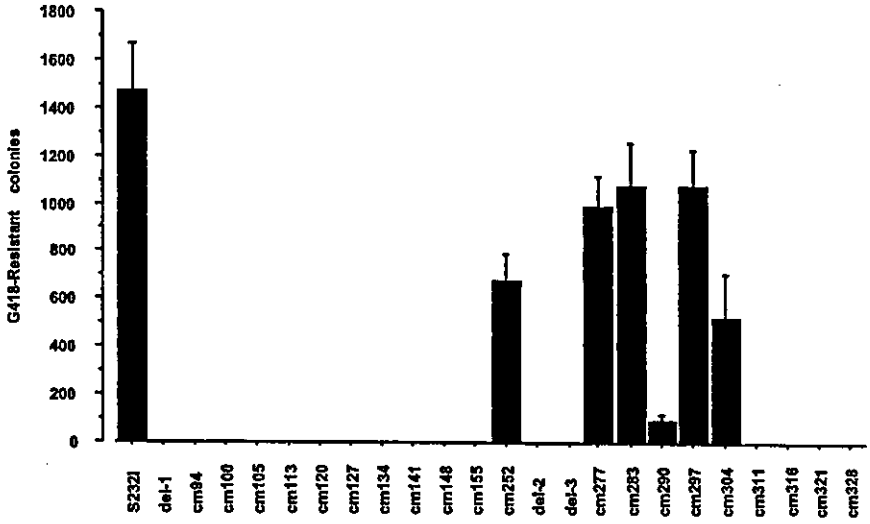

FIG. 7. Effect of M1LE/S232I plus internal deletion mutations or alanine-substitution mutations. Huh-7-DMB cells were transfected with 1 μg of in vitro-transcribed M1LE/S232I plus 5Adel-1, 5Adel-2, 5Adel-3, and cm 94, 100, 105, 113, 120, 127, 134, 141, 148, 155, 252, 277, 283, 290, 297, 304, 311, 316, 321, and 328 RNA. G418-resistant cells were selected with a G418 concentration of 1 mg/ml and stained 4 weeks after transfection. This figure shows the mean number of G418-resistant cell colonies isolated per 10-cm-diameter cell culture dish per 1 μg of RNA. Error bars indicate the standard deviations of the results from at least three independent experiments. The number of G418-resistant cell colonies in M1LE/S232I is derived from the results shown in Fig. 6A.

replication complex. Alternatively, it cannot be excluded that the internal deletion and cm mutants may be defective in other unknown function(s) essential for HCV RNA replication.

Adaptive mutations that increase the efficiency of HCV RNA replication have been accumulated in different HCV replicon systems (4, 24, 35, 37, 40). We introduced several point mutations into NS5A of M1LE and found that two, S232I and S225P, positively affected colony formation as adaptive mutations in two different Huh-7 sublines. Interestingly, a deletion of S229 had an effect distinct from those of the other two mutations, since it was only effective in the cured cells, the KV-C subline. Also, it is noteworthy that wild-type M1LE could not replicate in the Huh-7-KV-C subline. The effect of the deletion of S229 and the replication incompetence of wild-type M1LE may be of interest for the elucidation of the phenotypic or genetic change(s) in the cured cells. In combination with the adaptive mutation, the deletion and cm mutants exhibited distinct phenotypes in HCV RNA replication.

First, the mutant missing region 3 was replication incompetent in the presence of S232I or S225P, which was in contrast

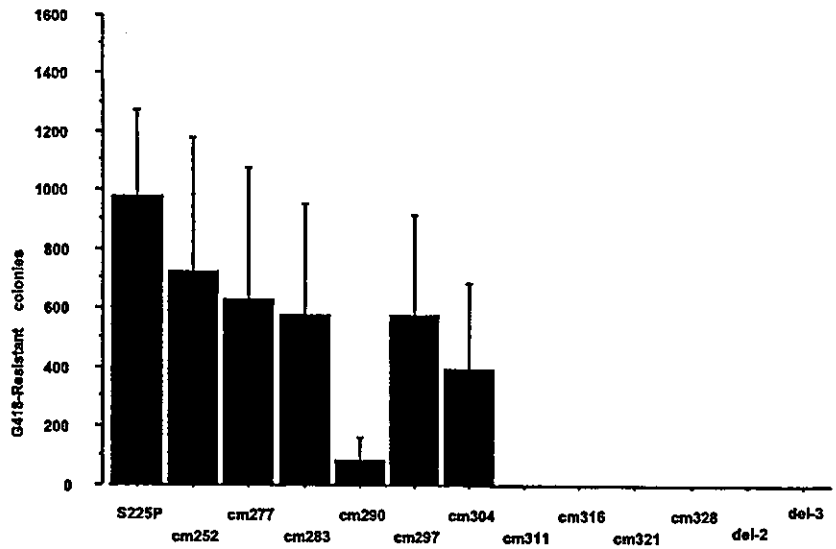

FIG. 8. Effect of M1LE/S225P plus internal deletion mutations or alanine-substitution mutations. Huh-7-DMB cells were transfected with 1 μg of in vitro-transcribed M1LE/S225P plus 5Adel-2, 5Adel-3, and cm 252, 277, 283, 290, 297, 304, 311, 316, 321, and 328 RNA. G418-resistant cells were selected with a G418 concentration of 1 mg/ml and stained 4 weeks after transfection. This figure shows the mean number of G418-resistant cell colonies isolated per 10-cm-diameter cell culture dish per 1 μg of RNA. Error bars indicate the standard deviations of the results from at least three independent experiments. The number of G418-resistant cell colonies in M1LE/S225P is derived from the results shown in Fig. 6A.

to the dramatic increase in HCV RNA replication efficiency obtained by introducing the adaptive mutation alone. A similar but more moderate phenotype was observed with cm 252 when the adaptive mutation was present. Our result is different from the reported enhancement of G418-resistant colony formation caused by a large 47-aa deletion in HCV-Con1 (4) and by a natural 4-aa insertion in HCV-N (29). Region 3 contains the IFN sensitivity-determining region, within which mutations have been reported to be associated with sensitivity to IFN therapy in patients with chronic HCV infection in Japan (14, 15). Region 3 is almost the same as a protein kinase R (PKR)-binding domain (18). It has been reported that NS5A can disrupt the dimerization of PKR through binding, resulting in the repression of PKR function, and efficient HCV RNA replication may involve a block in PKR-dependent signaling (18, 46). In this context, the adaptive mutations can greatly augment HCV RNA replication and thus may induce PKR, which could be inactivated via interaction with the PKR-binding region of NS5A, region 3, but not with those mutants defective in PKR-binding, such as del-3 and cm 252.

Second, cm 290 was less replication competent than the other cm mutants in region 2 when the adaptive mutation, S2321 or S225P, was present. The highly charged sequence mutated in cm 290 may be critical for HCV RNA replication in the presence of the adaptive mutation. To address this point, four different combinations of three to four alanine substitutions in 7 aa residues were introduced into the M1LE/S2321 construct. All of these mutants were more efficient in HCV RNA replication than M1LE/S2321 plus cm 290 but still less so than the other replication-competent mutants in region 2 (data not shown), suggesting that all or most amino acids in the sequence contribute to its critical role in HCV RNA replication in the presence of the adaptive mutations. This result may suggest a functional linkage of the sequence mutated in cm 290 to the adaptive mutations.

In HCV subgenomic replicons, some groups have found that cured cell clones showed a high permissiveness for HCV RNA replication (5, 45) while another has not (40). Between the recipient sublines we used, the cured cells (Huh-7-KV-C) shared the nonpermissive property for wild-type M1LE; however, the DMB subline was permissive for wild-type M1LE and/or adaptive mutations with lower efficiency than the KV-C subline. These results suggest that several different genetic or phenotypic alterations in recipient cells emerge under IFN treatment or multiple ways for cells to be permissive to HCV RNA replication.

In summary, we established a highly efficient HCV replicon system derived from the isolate M1LE and demonstrated that the two regions critical for the interaction between NS5A and NS5B are also indispensable for HCV RNA replication in an HCV replicon system. Our results strongly suggest that NS5A is involved in the HCV replication complex and acts as a positive modulator of HCV RNA replication through its interaction with NS5B. The molecular mechanism of this positive effect by NS5A remains to be elucidated and may lead to the design of new drugs that inhibit HCV RNA replication.

ACKNOWLEDGMENTS

We are grateful to N. Hayashi and T. Nomura for encouraging discussion. We also thank M. Yasukawa and K. Kuwabara for technical assistance.

This work was supported in part by the Program for Promotion of Fundamental Studies in Health Sciences of the Organization for Pharmaceutical Safety and Research, Grants-in-aid for scientific research (B) and development, and Grants-in-aid for scientific research on priority areas (C) in oncogenesis from the Ministry of Education, Sports, Culture, and Technology.

REFERENCES

1. **Alter, H. J., R. H. Purcell, J. W. Shih, J. C. Melpolder, M. Houghton, Q. L. Choo, and G. Kuo.** 1989. Detection of antibody to hepatitis C virus in prospectively followed transfusion recipients with acute and chronic non-A, non-B hepatitis. N. Engl. J. Med. 321:1494–1500.
2. **Bartenschlager, R., L. Ahlborn-Laake, J. Mous, and H. Jacobsen.** 1993. Nonstructural protein 3 of the hepatitis C virus encodes a serine-type proteinase required for cleavage at the NS3/4 and NS4/5 junctions. J. Virol. 67:3835–3844.
3. **Behrens, S. E., L. Tomei, and R. De Francesco.** 1996. Identification and properties of the RNA-dependent RNA polymerase of hepatitis C virus. EMBO J. 15:12–22.
4. **Blight, K. J., A. A. Kolykhalov, and C. M. Rice.** 2000. Efficient initiation of HCV RNA replication in cell culture. Science 290:1972–1974.
5. **Blight, K. J., J. A. McKeating, and C. M. Rice.** 2002. Highly permissive cell lines for subgenomic and genomic hepatitis C virus RNA replication. J. Virol. 76:13001–13014.
6. **Blight, K. J., J. A. McKeating, J. Marcotrigiano, and C. M. Rice.** 2003. Efficient replication of hepatitis C virus genotype 1a RNAs in cell culture. J. Virol. 77:3181–3190.
7. **Bordo, D., and P. Argos.** 1991. Suggestion for safe residue substitutions in site-directed mutagenesis. J. Mol. Biol. 217:721–729.
8. **Brass, V., E. Bieck, R. Montserret, B. Wölk, J. A. Hellings, H. E. Blum, F. Penin, and D. Moradpour.** 2002. An amino-terminal amphipathic α-helix mediates membrane association of the hepatitis C virus nonstructural protein 5A. J. Biol. Chem. 277:8130–8139.
9. **Choo, Q. L., G. Kuo, A. J. Weiner, L. R. Overby, D. W. Bradley, and M. Houghton.** 1989. Isolation of a cDNA clone derived from a blood-borne non-A, non-B viral hepatitis genome. Science 244:359–362.
10. **Chung, K. M., J. Lee, J. E. Kim, O. K. Song, S. Cho, J. Lim, M. Seedorf, B. Hahm, and S. K. Jang.** 2000. Nonstructural protein 5A of hepatitis C virus inhibits the function of karyopherin β3. J. Virol. 74:5233–5241.
11. **Dimitrova, M., I. Imbert, M. P. Kieney, and C. Schuster.** 2003. Protein-protein interactions between hepatitis C virus nonstructural proteins. J. Virol. 77:5401–5414.
12. **Egger, D., B. Wölk, R. Gosert, L. Bianchi, H. E. Blum, D. Moradpour, and K. Bienz.** 2002. Expression of hepatitis C virus proteins induces distinct membrane alterations including a candidate viral replication complex. J. Virol. 76:5974–5984.
13. **Elazar, M., K. H. Cheong, P. Liu, H. B. Greenberg, C. M. Rice, and J. S. Glenn.** 2003. Amphipathic helix-dependent localization of NS5A mediates hepatitis C virus RNA replication. J. Virol. 77:6055–6061.
14. **Enomoto, N., I. Sakuma, Y. Asahina, M. Kurosaki, T. Murakami, C. Yamamoto, N. Izumi, F. Marumo, and C. Sato.** 1995. Comparison of full-length sequence of interferon-sensitive and resistant hepatitis C virus 1b. Sensitivity to interferon is conferred by amino acid substitutions in the NS5A region. J. Clin. Investig. 96:224–230.
15. **Enomoto, N., I. Sakuma, Y. Asahina, M. Kurosaki, T. Murakami, C. Yamamoto, Y. Ogura, N. Izumi, F. Marumo, and C. Sato.** 1996. Mutations in the nonstructural protein 5A gene and response to interferon in patients with chronic hepatitis C virus 1b infection. N. Engl. J. Med. 334:77–82.
16. **Ferrari, E., J. Wright-Minogue, J. W. S. Fang, B. M. Baroudy, J. Y. N. Lau, and Z. Hong.** 1999. Characterization of soluble hepatitis C virus RNA-dependent RNA polymerase expressed in *Escherichia coli*. J. Virol. 73:1649–1654.
17. **Friebe, P., and R. Bartenschlager.** 2002. Genetic analysis of sequence in the 3′ nontranslated region of hepatitis C virus that are important for RNA replication. J. Virol. 76:5326–5338.
18. **Gale, M., Jr., C. M. Blakely, B. Kwieciszewski, S. L. Tan, M. Dossett, N. M. Tang, M. J. Korth, S. J. Polyak, D. R. Gretch, and M. G. Katze.** 1998. Control of PKR protein kinase by hepatitis C virus nonstructural 5A protein: molecular mechanisms of kinase regulation. Mol. Cell. Biol. 18:5208–5218.
19. **Ghosh, A. K., M. Majumder, R. Steele, P. Yaciuk, J. Chrivia, R. Ray, and R. B. Ray.** 2000. Hepatitis C virus NS5A protein modulates transcription through a novel cellular transcription factor SRCAP. J. Biol. Chem. 275: 7184–7188.
20. **Gosert, R., D. Egger, V. Lohmann, R. Bartenschlager, H. E. Blum, K. Bienz, and D. Moradpour.** 2003. Identification of the hepatitis C virus RNA replication complex in Huh-7 cells harboring subgenomic replicons. J. Virol. 77:5487–5492.
21. **Grakoui, A., D. W. McCourt, C. Wychowski, S. M. Feinstone, and C. M. Rice.** 1993. Characterization of the hepatitis C virus-encoded serine protease: determination of proteinase-dependent polyprotein cleavage sites. J. Virol. 67:2832–2843.
22. **Grakoui, A., C. Wychowski, C. Lin, S. M. Feinstone, and C. M. Rice.** 1993.

Expression and identification of hepatitis C virus polyprotein cleavage products. J. Virol. 67:1385–1395.
23. Gu, B., A. T. Gates, O. Isken, S. E. Behrens, and R. T. Sarisky. 2003. Replication studies using genotype 1a subgenomic hepatitis C virus replicons. J. Virol. 77:5352–5359.
24. Guo, J. T., V. V. Bichko, and C. Seeger. 2001. Effect of alpha interferon on the hepatitis C virus replicon. J. Virol. 75:8516–8523.
25. Hijikata, M., H. Mizushima, Y. Tanji, Y. Komoda, Y. Hirowatari, T. Akagi, N.Kato, K. Kimura, and K. Shimotohno. 1993. Proteolytic processing and membrane association of putative nonstructural proteins of hepatitis C virus. Proc. Natl. Acad. Sci. USA 90:10773–10777.
26. Hijikata, M., N. Kato, Y. Ootsuyama, M. Nakagawa, and K. Shimotohno. 1991. Gene mapping of the putative structural region of the hepatitis C virus genome by *in vitro* processing analysis. Proc. Natl. Acad. Sci. USA 88:5547–5551.
27. Hijikata, M., N. Kato, Y. Ootsuyama, M. Nakagawa, S. Ohkoshi, and K. Shimotohno. 1991. Hypervariable regions in the putative glycoprotein of hepatitis C virus. Biochem. Biophys. Res. Commun. 175:220–228.
28. Hügle, T., F. Fehrmann, E. Bieck, M. Kohara, H. G. Kräusslich, C. M. Rice, H. E. Blum, and D. Moradpour. 2001. The hepatitis C virus nonstructural protein 4B is an integral endoplasmic reticulum membrane protein. Virology 284:70–81.
29. Ikeda, M., M. Yi, K. Li, and S. M. Lemon. 2002. Selectable subgenomic and genome-length dicistronic RNAs derived from an infectious molecular clone of the HCV-N strain of hepatitis C virus replicate efficiently in cultured Huh7 cells. J. Virol. 76:2997–3006.
30. Ivashkina, N., B. Wölk, V. Lohmann, R. Bartenschlager, H. E. Blum, F. Penin, and D. Moradpour. 2002. The hepatitis C virus RNA-dependent RNA polymerase membrane insertion sequence is a transmembrane segment. J. Virol. 76:13088–13093.
31. Kato, N., T. Nakazawa, T. Mizutani, and K. Shimotohno. 1995. Susceptibility of human T-lymphotropic virus type I-infected cell line MT-2 to hepatitis C virus infection. Biochem. Biophys. Res. Commun. 206:863–869.
32. Kato, N., Y. Ootsuyama, H. Sekiya, S. Ohkoshi, T. Nakazawa, M. Hijikata, and K. Shimotohno. 1994. Genetic drift in hypervariable region 1 of the viral genome in persistent hepatitis C virus infection. J. Virol. 68:4776–4784.
33. Kishine, H., K. Sugiyama, M. Hijikata, N. Kato, H. Takahashi, T. Noshi, Y. Nio, M. Hosaka, Y. Miyanari, and K. Shimotohno. 2002. Subgenomic replicon derived from a cell line infected with the hepatitis C virus. Biochem. Biophys. Res. Commun. 293:993–999.
34. Kolykhalov, A. A., K. Mihalik, S. M. Feinstone, and C. M. Rice. 2000. Hepatitis C virus-encoded enzymatic activities and conserved RNA elements in the 3′ nontranslated region are essential for virus replication in vivo. J. Virol. 74:2046–2051.
35. Krieger, N., V. Lohmann., and R. Bartenschlager. 2001. Enhancement of hepatitis C virus RNA replication by cell culture-adaptive mutations. J. Virol. 75:4614–4624.
36. Lin, Y., H. Tang, T. Nomura, D. Dorjsuren, N. Hayashi, W. Wei, T. Ohta, R. Roeder, and S. Murakami. 1998. The hepatitis B virus X protein is a co-activator of activated transcription that modulates the transcription machinery and distal binding activators. J. Biol. Chem. 273:27097–27103.
37. Lohmann, V., F. Körner, A. Dobierzewska, and R. Bartenschlager. 2001. Mutations in hepatitis C virus RNAs conferring cell culture adaptation. J. Virol. 75:1437–1449.
38. Lohmann, V., F. Körner, J. O. Koch, U. Herian, L. Theilmann, and R. Bartenschlager. 1999. Replication of subgenomic hepatitis C virus RNAs in a hepatoma cell line. Science 285:110–113.
39. Lohmann, V., F. Körner, U. Herian, and R. Bartenschlager. 1997. Biochemical properties of hepatitis C virus NS5B RNA-dependent RNA polymerase and identification of amino acid sequence motifs essential for enzymatic activity. J. Virol. 71:8416–8428.
40. Lohmann, V., S. Hoffmann, U. Herian, F. Penin, and R. Bartenschlager. 2003. Viral and cellular determinants of hepatitis C virus RNA replication in cell culture. J. Virol. 77:3007–3019.
41. Major, M. E., and S. M. Feinstone. 1997. The molecular virology of hepatitis C. Hepatology 25:1527–1538.
42. Majumder, M., A. K. Ghosh, R. Steele, R. Ray, and R. B. Ray. 2001. Hepatitis C virus NS5A physically associates with p53 and regulates p21/waf1 gene expression in a p53-dependent manner. J. Virol. 75:1401–1407.
43. Mizutani, T., N. Kato, S. Saito, M. Ikeda, K. Sugiyama, and K. Shimotohno. 1996. Characterization of hepatitis C virus replication in cloned cells obtained from a human T-cell leukemia virus type 1-infected cell line, MT-2. J. Virol. 70:7219–7223.
44. Murphy, F. A., C. M. Fauquet, D. H. L. Bishop, S. A. Ghabrial, A. W. Jarvis, G. P. Martelli, M. A. Mayo, and M. D. Summers. 1995. Classification and nomenclature of viruses: sixth report of the internal committee on taxonomy of viruses, p. 424–426. Springer-Verlag, Vienna, Austria.
45. Murray, E. M., J. A. Grobler, E. J. Markel, M. F. Pagnoni, G. Paonessa, A. J. Simon, and O. A. Flores. 2003. Persistent replication of hepatitis C virus replicons expressing the β-lactamase reporter in subpopulations of highly permissive Huh7 cells. J. Virol. 77:2928–2935.
46. Pflugheber, J., B. Fredericksen, R. Sumpter, Jr., C. Wang, F. Ware, D. L. Sodora, and M. Gale, Jr. 2002. Regulation of PKR and IRF-1 during hepatitis C virus RNA replication. Proc. Natl. Acad. Sci. USA 99:4650–4655.
47. Piccininni, S., A. Varakliotl, M. Nardelli, B. Dave, K. D. Raney, and J. E. G. McCarthy. 2002. Modulation of the hepatitis C virus RNA-dependent RNA polymerase activity by the non-structural (NS) 3 helicase and the NS4B membrane protein. J. Biol. Chem. 277:45670–45679.
48. Qin, W., H. Luo, T. Nomura, N. Hayashi, T. Yamashita, and S. Murakami. 2002. Oligomeric interaction of hepatitis C virus NS5B is critical for catalytic activity of RNA-dependent RNA polymerase. J. Biol. Chem. 277:2132–2137.
49. Qin, W., T. Yamashita, Y. Shirota, Y. Lin, W. Wei, and S. Murakami. 2001. Mutational analysis of the structure and functions of hepatitis C virus RNA-dependent RNA polymerase. Hepatology 33:728–737.
50. Saito, I., T. Miyamura, A. Ohbayashi, H. Harada, T. Katayama, S. Kikuchi, Y. Watanabe, S. Koi, M. Onji, Y. Ohta, Q. Choo, M. Houghton, and G. Kuo. 1990. Hepatitis C virus infection is associated with the development of hepatocellular carcinoma. Proc. Natl. Acad. Sci. USA 87:6547–6549.
51. Santolini, E., L. Pacini, C. Fipaldini, G. Migliaccio, and N. Monica. 1995. The NS2 protein of hepatitis C virus is a transmembrane polypeptide. J. Virol. 69:7461–7471.
52. Schmidt-Mende, J., E. Bieck, T. Hügle, F. Penin, C. M. Rice, H. E. Blum, and D. Moradpour. 2001. Determinants for membrane association of the hepatitis C virus RNA-dependent RNA polymerase. J. Biol. Chem. 276:44052–44063.
53. Seeff, L. B. 1997. Natural history of hepatitis C. Hepatology 26:21S–28S.
54. Shirota, Y., H. Luo, W. Qin, S. Kaneko, T. Yamashita, K. Kobayashi, and S. Murakami. 2002. Hepatitis C virus (HCV) NS5A binds RNA-dependent RNA polymerase (RdRp) NS5B and modulates RNA-dependent RNA polymerase activity. J. Biol. Chem. 277:11149–11155.
55. Sugiyama, K., N. Kato, T. Mizutani, M. Ikeda, T. Tanaka, and K. Shimotohno. 1997. Genetic analysis of the hepatitis C virus (HCV) genome from HCV-infected human T cells. J. Gen. Virol. 78:329–336.
56. Tan, S. L., H. Nakao, Y. He, S. Vijaysri, P. Neddermann, B. L. Jacobs, B. J. Mayer, and M. G. Katze. 1999. NS5A, a nonstructural protein of hepatitis C virus, binds growth factor receptor-bound protein 2 adaptor protein in a Src homology 3 domain/ligand-dependent manner and perturbs mitogenic signaling. Proc. Natl. Acad. Sci. USA 96:5533–5538.
57. Tsukiyama-Kohara, K., N. Iizuka, M. Kohara, and A. Nomoto. 1992. Internal ribosome entry site within hepatitis C virus RNA. J. Virol. 66:1476–1483.
58. Tu, H., L. Gao, S. T. Shi, D. R. Taylor, T. Yang, A. K. Mircheff, Y. Wen, A. E. Gorbalenya, S. B. Hwang, and M. M. C. Lai. 1999. Hepatitis C virus RNA polymerase and NS5A Complex with a SNARE-like protein. Virology 263:30–41.
59. Wang, C., P. Sarnow, and A. Siddiqui. 1993. Translation of human hepatitis C virus RNA in cultured cells is mediated by internal ribosome-binding mechanism. J. Virol. 67:3338–3344.
60. Wang, Q. M., M. A. Hockman, K. Staschke, R. B. Johnson, K. A. Case, J. Lu, S. Parsons, F. Zhang, R. Rathnachalam, K. Kirkegaard, and J. M. Colacino. 2002. Oligomerization and cooperative RNA synthesis activity of hepatitis C virus RNA-dependent RNA polymerase. J. Virol. 76:3865–3872.
61. Weiner, A. J., H. M. Geysen, C. Christopherson, J. E. Hall, T. J. Mason, G. Saracco, F. Bonino, K. Crawford, C. D. Marion, K. A. Crawford, M. Brunetto, P. J. Barr, T. Miyamura, J. McHutchinson, and M. Houghton. 1992. Evidence for immune selection of hepatitis C virus (HCV) putative envelope glycoprotein variants: potential role in chronic HCV infections. Proc. Natl. Acad. Sci. USA 89:3468–3472.
62. Weiner, A. J., M. J. Brauer, J. Rosenblatt, K. H. Richman, J. Tung, K. Crawford, F. Bonino, G. Saracco, Q. L. Choo, M. Houghton, and J. H. Han. 1991. Variable and hypervariable domains are found in the regions of HCV corresponding to the flavivirus envelope and NS1 proteins and the pestivirus envelope glycoproteins. Virology 180:842–848.
63. Wölk, B., D. Sansonno, H. G. Kräusslich, F. Dammacco, C. M. Rice, H. E. Blum, and D. Moradpour. 2000. Subcellular localization, stability, and trans-cleavage competence of the hepatitis C virus NS3-NS4A complex expressed in tetracycline-regulated cell lines. J. Virol. 74:2293–2304.
64. Yamashita, T., S. Kaneko, Y. Shirota, W. Qin, T. Nomura, K. Kobayashi, and S. Murakami. 1998. RNA-dependent RNA polymerase activity of the soluble recombinant hepatitis C virus NS5B protein truncated at the C-terminal region. J. Biol. Chem. 273:15479–15486.
65. Yanagi, M., M. St. Claire, S. U. Emerson, R. H. Purcell, and J. Bukh. 1999. *In vivo* analysis of the 3′ untranslated region of the hepatitis C virus after *in vitro* mutagenesis of an infectious cDNA clone. Proc. Natl. Acad. Sci. USA 96:2291–2295.
66. Yi, M., and S. M. Lemon. 2003. 3′ Nontranslated RNA signals required for replication of hepatitis C virus RNA. J. Virol. 77:3557–3568.
67. Zech, B., A. Kurtenbach, N. Krieger, D. Strand, S. Blencke, M. Morbitzer, K. Salassidis, M. Cotten, J. Wissing, S. Obert, R. Bartenschlager, T. Herget, and H. Daub. 2003. Identification and characterization of amphiphysin II as a novel cellular interaction partner of the hepatitis C virus NS5A protein. J. Gen. Virol. 84:555–560.

Available online at www.sciencedirect.com
SCIENCE DIRECT®
Biochemical and Biophysical Research Communications 315 (2004) 1088–1096
BBRC
www.elsevier.com/locate/ybbrc

A low-density cDNA microarray with a unique reference RNA: pattern recognition analysis for IFN efficacy prediction to HCV as a model☆

Akito Daiba,[a] Niro Inaba,[a] Satoshi Ando,[a] Naoki Kajiyama,[a] Hiroshi Yatsuhashi,[b] Hiroshi Terasaki,[a] Atsushi Ito,[a] Masanori Ogasawara,[a] Aki Abe,[a] Junichi Yoshioka,[a] Kazuhiro Hayashida,[c,1] Shuichi Kaneko,[d] Michinori Kohara,[e] and Satoru Ito[a,*,2]

[a] *JGS Japan Genome Solutions, Inc. 51 Komiya-cho, Hachioji, Tokyo 192-0031, Japan*
[b] *National Nagasaki Medical Center, Kubara 2-1001-1 Omura City, Nagasaki 856-8562, Japan*
[c] *Medicine and Biosystemic Science, Kyushu University Graduate School of Medical Sciences, 3-1-1 Maidashi, Higashi-ku, Fukuoka 812-8582, Japan*
[d] *Kanazawa University Graduate School of Medical Sciences, 13-1 Muro-machi, Kanazawa 920-8641, Japan*
[e] *Tokyo Metropolitan Institute of Medical Science, 3-18-22 Hon-komagome, Bunkyo-ku, Tokyo 113-8613, Japan*

Received 9 January 2004

Abstract

We have designed and established a low-density (295 genes) cDNA microarray for the prediction of IFN efficacy in hepatitis C patients. To obtain a precise and consistent microarray data, we collected a data set from three spots for each gene (mRNA) and using three different scanning conditions. We also established an artificial reference RNA representing pseudo-inflammatory conditions from established hepatocyte cell lines supplemented with synthetic RNAs to 48 inflammatory genes. We also developed a novel algorithm that replaces the standard hierarchical-clustering method and allows handling of the large data set with ease. This algorithm utilizes a standard space database (SSDB) as a key scale to calculate the Mahalanobis distance (MD) from the center of gravity in the SSDB. We further utilized sMD (divided by parameter k: MD/k) to reduce MD number as a predictive value. The efficacy prediction of conventional IFN mono-therapy was 100% for non-responder (NR) vs. transient responder (TR)/sustained responder (SR) ($P < 0.0005$). Finally, we show that this method is acceptable for clinical application.

Keywords: Low-density microarray; Artificial reference RNA; Efficacy prediction; Mahalanobis distance

Large data sets can be collected from cDNA microarrays for the study of expression profiles in biological systems. The large amount of data generated can be especially useful to help cluster genes into interest groups. Such genome-wide information can be used for clinical applications (see reviews, [1–5]), for example, for the identification of the cDNA expression patterns associated with different stages of tumor development. However, translating complex microarray data into practical clinical applications has been difficult. New algorithms are being developed to solve this problem, for example for the prognosis of cancer treatment [6,7]. Also, low-density microarrays with selected genes of interest can simplify the analysis of microarray data.

Another critical issue in understanding microarray data is the level of precision in the data set. Solid phase DNA hybridization is not as quantitative as hybridization in solution, and scanners have limited dynamic

☆ *Abbreviations:* SAGE, serial analysis of gene expression; SSDB, standard space database; MD, Mahalanobis distance; sMD, scaled MD; FL, firefly luciferase gene; RL, *Renilla* luciferase gene; GP, baculovirus glycoprotein gene; LD, lambda DNA; MEP, microcapillary electrophoretic; aRNA, amplified RNA; NR, non-responder; SR, sustained responder; TR, transient responder.

* Corresponding author. Fax: +81-426-45-0461.
E-mail address: sr-itou@jgs-inc.co.jp (S. Ito).
[1] Present address: Sasebo Kyosai Hospital, 10-17 Shimaji, Sasebo, Nagasaki 857-8575, Japan.
[2] Visiting position: Medical Research Institute, Tokyo Medical and Dental University.

0006-291X/$ - see front matter © 2004 Elsevier Inc. All rights reserved.
doi:10.1016/j.bbrc.2004.01.160

ranges. In addition, sample variability can result from variations in sampling conditions, RNA amplification, RNA degradation, and cDNA labeling conditions. These factors are not well understood, and, currently, precision is primarily controlled at the level of data collection [8–10].

One means of enhancing the precision of data collection is to use reference controls for each individual. This can be accomplished by laser-captured microdissection of tissues into diseased and counter part areas [11,12]. In case of hepatitis C, this is difficult because inflammatory damage occurs throughout the liver. Another possible approach is to utilize artificial reference RNAs as a reference [13–15] in conjunction with RNA from established cell lines, such as hepatocellular carcinoma cell lines. However, the stages and characteristics of the disease in vivo and in vitro can differ, and expression of some RNAs of interest, especially some inflammatory genes, may be too low in the cultured cells to produce a satisfactory signal-to-noise ratio.

In the current studies, we identified inflammatory genes that can be used for a low-density microarray to predict the efficacy of INF treatment in hepatitis C patients. We found sufficient levels of expression for these genes in patient samples, but very low levels of expression in established cell lines. We overcame this problem by using a low-density cDNA microarray system in conjunction with a unique artificial reference RNA. In addition, we describe an algorithm for analysis of the microarray data.

Methods

cDNA Microarray. We selected 295 genes for the cDNA microarray based on publicly available data, including SAGE analysis and other DNA microarray data from HCV patients and a normal subject [16,17]. From 2000 candidate genes, we omitted low frequency-tag genes based on the SAGE data. Genes previously identified as predictive host factors for IFN efficacy [18–20] were given a high priority. For most of the genes, each cDNA was designed approximately 500–600 bp and within approximately 1 kb region from the 3′-poly(A) tail and all cDNAs for microarray probe were cloned into the pGEM vector (Promega, Madison, WI). We also selected and cloned external control genes (approximately 0.5–1 kb) into the pGEM vector to establish the dynamic range of the microarray. These genes were firefly luciferase (FL; negative control), *Renilla* luciferase (RL) [21], baculovirus envelope gp64 (GP), and lambda phage DNA (LD). All clones for capture probe on microarray were sequenced and validated by comparison with the GenBank sequence. The aminosilane surfaces of SuperAmine glass slides (TeleChem International, Sunnyvale, CA) were stamped with triplicate spots of cDNA probe corresponding to each of the remaining 295 genes. The average spot size was 150 μm and separated each other with a distance (500 μm) as shown in Fig. 2B.

Reference RNA preparation. Extracted total RNAs from four hepatocellular carcinoma cell lines (HepG2, Hep3B, Huh7, and IMY-4 [22]) purified through RNeasy column (Qiagen, Hilden, Germany) were mixed as a reference source. In order to find a mixing ratio of four cell derived RNAs and provide reliable reference source, we measured the copy number of certain genes in each cell line by real-time PCR method. Using real-time PCR with the PRISM 7900HT system (Applied Biosystems, Foster City, CA), we measured the copy number of several genes, including the IFN-α/β receptor, double-strand RNA-activated protein kinase (PKR), 2′,5′-oligoadenylate synthetase (2,5-AS), interferon regulatory factor-1 (IRF-1), interferon regulatory factor-3 (IRF-3), and glyceraldehyde-3-phosphate dehydrogenase (GAPDH). The primer sets were as follows: IFN-α/β receptor (forward: GTGACCTCACAGATGAGTGG; reverse: CCCTCTGA CTGTTCTTCAATGA; and probe: CACCGTCCTAGAAGGA TTCAGCGG), PKR (forward: CCTGTCCTCTGGTTCTTTTG; reverse: TGTCAGGAAGGTCAAATCTG; and probe: CTACGTGT GAGTCCCAAAGCAAC), 2,5-AS (forward: CTCAGAAATAC CCCAGCCAAATC; reverse: GTGGTGAGAGGACTGAGGAA; and probe: CCAGGTCAGCGTCAGATCGGCCTC), IRF-1 (forward: GCAAGGCCAAGAGGAAGTCA; reverse: TCATCAGG CAGAGTGGAGCT; and probe: TTCCAGCCCTGATACCTTC TCTGATGG), IRF-3 (forward: AAGGAAGGAGGCGTGTTTGA; reverse: ATTTCTACCAAGGCCCTGAGG; and probe: CGTCCGC TTCCTTCCGTGAAGGTAAT), GAPDH (forward: GAAGGTGA AGGTCGGAGT; reverse: GAAGATGGTGATGGGATTTC; and probe: CAAGCTTCCCGTTCTCAGCC). The RNA mixture was amplified using MessageAmp aRNA kit (Ambion, Austin, TX). The resulting aRNA was used as the reference aRNA. Moreover, we cloned genes (RL, GP, and LD; ~1000 bp) into pCRII TOPO vector (Invitrogen, Carlsbad, CA) as scanning range markers as well as 48 genes (in the same TOPO vector) of inflammatory genes to spike into reference aRNA. Each cloning region was designed to be larger than the size of capture probes on the microarray. Then three external control RNAs and additional spike RNAs of 48 genes were synthesized by Megascript T7 kit (Ambion, Austin, TX). Three external control RNAs were mixed as spike control mixture in both target sample and reference aRNAs. Other 48 spike RNAs were added to the reference aRNA.

Sample RNA preparation, labeling, hybridization, and scanning. Total RNA of liver biopsy samples was isolated by Isogen (Nippon Gene, Tokyo, Japan) extraction according to manufacturer's instruction. The total RNA quality was confirmed with a Bioanalyser 2100 microcapillary-electrophoretic (MEP) analyzer (Agilent Technologies, Palo Alto, CA). The 28S/18S ratio of the total RNA was >1.0. Then total RNA (1–2 μg) was transcribed and amplified to produce amplified sample RNA (aRNA) using the MessageAmp aRNA kit (Ambion, Austin, TX) according to manufacturer's instructions. Next, an external control RNA mixture (LD, GP, and RL) was added to both the sample and reference aRNAs. These mixed sample and reference aRNAs were labeled using SuperScript II kit with random hexamer (TaKaRa, Kyoto, Japan) with Cy3-dUTP and Cy5-dUTP (Perkin–Elmer, Boston, MA), respectively. Competitive hybridization of Cy3-labeled sample and Cy5-labeled reference cDNAs on the microarray was carried out according to Brown and coworkers [23]. Slides were scanned three times with ScanArray 5000 (Perkin–Elmer, Boston, MA). Each scan was carried out using the external spike level around 30,000. The data were converted from tif image data to signal using ImaGene software (BioDiscovery, El Segundo, CA) for further statistical analysis. Three file data of each three spot data of each gene were merged to establish the single representative data for each gene (Patent pending: PCT/JP03/06677). The Cy3 (patient sample)/Cy5 (reference sample) ratio of each mRNA signal was calculated for further analysis.

Patients. Liver biopsy samples from five patients receiving IFN-α monotherapy and 10 patients receiving a combination therapy (a mixture of IFN-α, IFN-β, and IFN-α/β) were obtained during 1992–2000 from Kyushu University Hospital and Nagasaki National Medical Center, respectively. Biopsy samples were stored at −80 °C. Informed consent was obtained from all patients in accordance with the Helsinki protocol. The samples were classified into three groups: sustained responders (SR) had an absence of serum HCV RNA both during the therapy and 6 months after the completion of therapy, non-responders (NR) were positive for serum HCV RNA during the

therapy, and transient responders (TR) had an absence of serum HCV RNA during the therapy or at the end of IFN treatment, but has serum HCV RNA after cessation of the therapy. Because RNA degradation may have occurred during storage, and because this can be a major source of variation in microarray data [24], we verified the quality of the extracted RNA by assessing the ribosomal RNA 28S/18S ratio.

Statistical data analysis. The merged data were subjected for hierarchical clustering to noise reduction and normalization (patent pending, PCT/JP03/06677) using the reference control and then analyzed with Genomic Profiler software (Mitsui Knowledge Industry, Tokyo, Japan). In addition, we developed a novel algorithm to calculate the Mahalanobis distance (MD) for the data from 15 patients using a standard space database (SSDB) (Eqs. (1)–(5) and Fig. 1). To establish the SSDB, we searched a gene set representing the differences between the SR/TR and NR groups. The necessary genes for the SSDB and MD calculations were selected using MATLAB (MathWorks, Natick, MA). We have calculated a graded scale utilizing variance–covariance to valuate dispersion and correlation of the standard group as a training set to establish the center of the gravity of SSDB. Once the SSDB was established, new test sample data were applied to the equations to calculate the MD. We utilize sMD as a predictive value. The sMD was presented from the center of gravity of SSDB (0:zero) along its scale to theoretically ∞. This method is one of the pattern recognition analysis dealing with correlation of multi-parameters [25].

$$d_{xi} = \frac{D_{xi} - \overline{D_x}}{\sigma_x} \quad \text{(auto scale)}, \quad (1)$$

$$S_{xx'} = \frac{\sum_{i=1}^{n} (d_{xi} - \overline{d_x})(d_{x'i} - \overline{d_{x'}})}{n-1} \quad \text{(variance–covariance)}, \quad (2)$$

$$S = \begin{bmatrix} S_{11} & S_{12} & \cdots & S_{1(k-1)} & S_{1k} \\ S_{21} & S_{22} & \cdots & S_{2(k-1)} & S_{2k} \\ \vdots & \vdots & \vdots & \vdots & \vdots \\ S_{(k-1)1} & S_{(k-1)2} & \cdots & S_{(k-1)(k-1)} & S_{(k-1)k} \\ S_{k1} & S_{k2} & \cdots & S_{k(k-1)} & S_{kk} \end{bmatrix} \quad \text{(variance–covariance matrix)}, \quad (3)$$

$$\mathrm{MD}^2 = [d_1 \ \cdots \ d_k] S^{-1} \begin{bmatrix} d_1 \\ \vdots \\ d_k \end{bmatrix} \quad \text{(Mahalanobis distance)}, \quad (4)$$

$$\mathrm{sMD} = \frac{\mathrm{MD}^2}{k} \quad \text{(scaled Mahalanobis distance)}. \quad (5)$$

Results and discussion

The low-density cDNA microarray

High-density microarray data were so hard to handle its huge data for analysis and difficult to understand their meaning. One approach is to minimize gene set for collection of mRNA profiling data to each category of research field. Chang et al. [26] have described the selection of data from high-density microarrays for prediction of "docetaxel" therapy efficacy of breast cancer. Specifically, they omitted low level signals of genes from the high-density microarray data at first. We followed a similar approach to select genes on our microarray, also omitting low frequency tag genes from the SAGE data. This ensured a steady state signal amongst the target samples. Based on this selection, we chose 295 genes for a low-density microarray system. The DNA sequence of each cloned gene fragment (500–600 bp) was validated by comparison with the published sequences in the GenBank database. To provide replicate data, the cDNAs were spotted in triplicate on the aminosilane-coated slide glass [8]. Scanning electron microscopy confirmed that the spots were round, smooth, and homogeneous without any doughnut features (Fig. 2). To obtain stable signals, we used three independent internal RNA references, including RL for the high expression range, GP for the middle range, and LD for the low range. The signals from the microarray were adjusted so that the ScanArray would give reliable signal of 30,000, which should be within the linear and stable range of the scanner (maximum signal = 65,535). We also carried out noise reduction and normalization of data using the artificial external spike genes as well as some housekeeping genes. Validation of the low-density cDNA microarray system was carried out using the RNA from HepG2 (data not shown).

Adjustment of reference RNA

Selection of an appropriate control reference is another important factor for accuracy in microarray analysis. One method has been to use laser microdissection to select normal tissue from the same patient as a reference. Although this is useful for single patients, it cannot be applied to comparison of multiple patients' samples because the baseline expression of specific genes can vary from patient to patient. Therefore, conditions including the duration of disease, the medications used, sampling conditions, storage conditions, and life style differences can cause variability in the microarray data. To eliminate this problem, we have used an artificial reference RNA isolated from cell lines as a reference. When we screened the signal levels of both reference and patient samples, we found 48 genes out of 295 genes in the microarray that were expressed in the patients but not or background level in the RNA mixture from the four cell lines. Typical data from the four cell reference mixture are shown in Fig. 3A. The IFN-receptor and some other well-known IFN-inducible factors are indicated. The graph shows that the levels of these mRNAs are in the low signal range. This includes the IFN-α/β receptor, even though it has been proposed as a possible marker for the prediction of IFN efficacy [18,19]. The problem in this case appears to be high variability in IFN-α/β receptor gene expression between different reference RNA preparations. To avoid this problem, we produced a large single preparation of reference RNA for future analyses. In addition, we have produced 48 synthetic RNAs, which we added to the reference RNA mixture. These synthetic RNAs were designed to be larger than the size of the capture probes on the microarray. The design and purity of some these synthetic

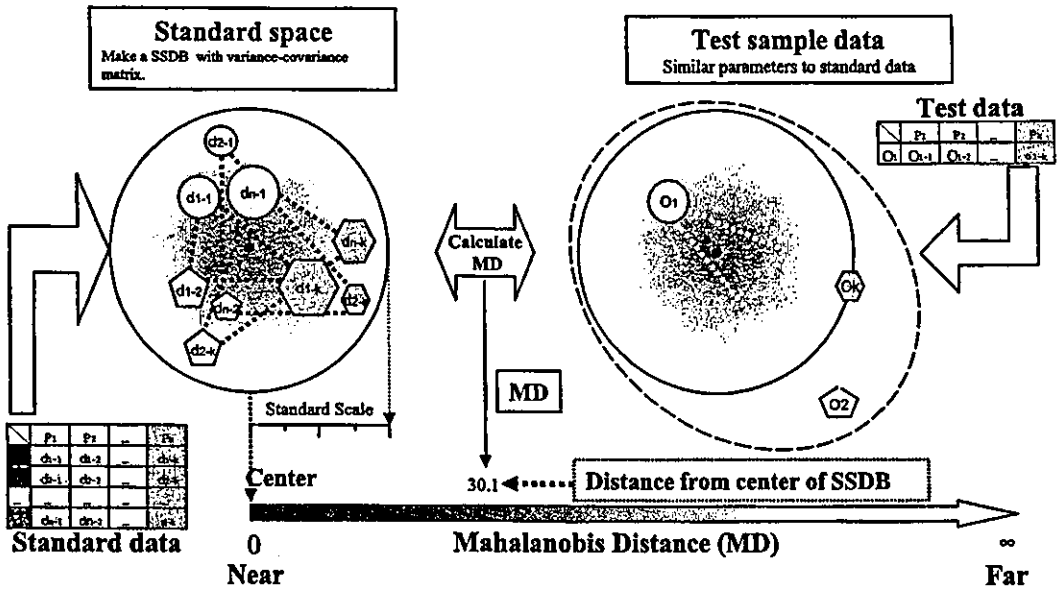

Fig. 1. Pattern recognition for establishment of SSDB and MD calculations. The standard space database (SSDB) was established based on a training data set. The parameter (1 to k) represents each data point (signal level for each gene) in the patient sample. A second parameter (1 to n) represents each patient. Both parameters were utilized along with the distinguishing genes for each group that were used in a variance–covariance matrix calculation to create the SSDB. Next, the test sample data were calculated to obtain the Mahalanobis distance (MD), where the MD represents the distance of new test sample data from the center of gravity in the SSDB. In theory, MD can be from 0 to ∞. A high MD value means that its distance is far away from the SSDB center of gravity.

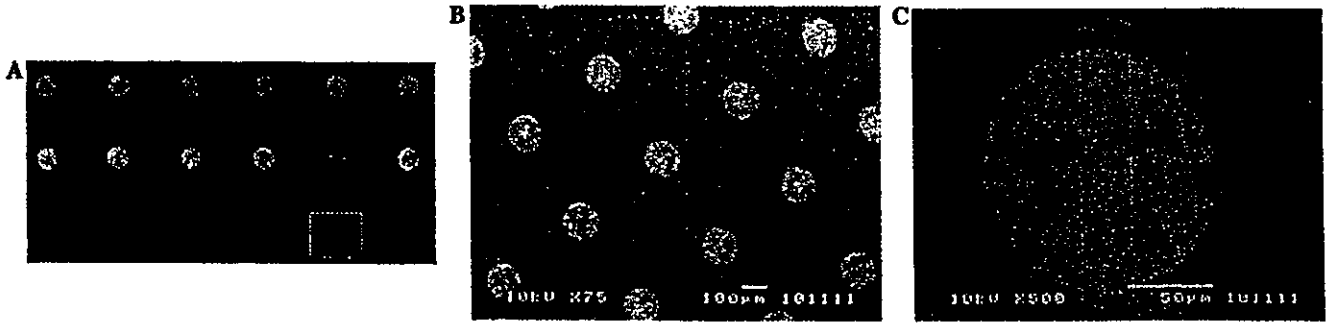

Fig. 2. Spot geometry on the cDNA microarray. (A) A typical fluorescent image was presented. The negative control (firefly luciferase) gene was spotted inside of the white square. Scanning electron microscopic images at (B) low power (75×) and (C) higher power (500×) are shown.

RNAs is shown in Fig. 3B. The level of the synthetic reference RNAs is shown as a scatter plot in Fig. 3C. These results show that the level of the synthetic RNA corresponds to the range of pseudo-inflammatory conditions. Thus, we spiked these 48 synthetic RNAs to the average signal level of patients which was surveyed at first. Without this synthetic reference RNA, it would be difficult to analyze and categorize the microarray data and use it to predict the efficacy of IFN treatment. Thus, the signal below the negative cut-off level will be treated as zero for further ratio calculation leads to nonsense.

Statistical analysis

A variety of normalization techniques have been used for the analysis of DNA microarray data [9,27–30]. Many of these techniques rely on the expression of housekeeping genes. However, it is difficult to find suitable candidates, and it would be difficult to integrate a large set of housekeeping genes onto the low-density cDNA microarray [30–32]. For these reasons, we have added synthetic non-human genes as external controls. We have also utilized some type of housekeeping genes for normalization of the microarray data (patent pending, PCT/JP03/06677). Furthermore, to minimize variability in the calculations due to variability in the fluorescence measurements, we used six data files (three scans of each Cy3/Cy5 wavelength) to merge into a single representative data for each gene expression analysis.

Hierarchical clustering by the classical method

Hierarchical clustering of the merged data was carried out using Euclid distance and Ward method with

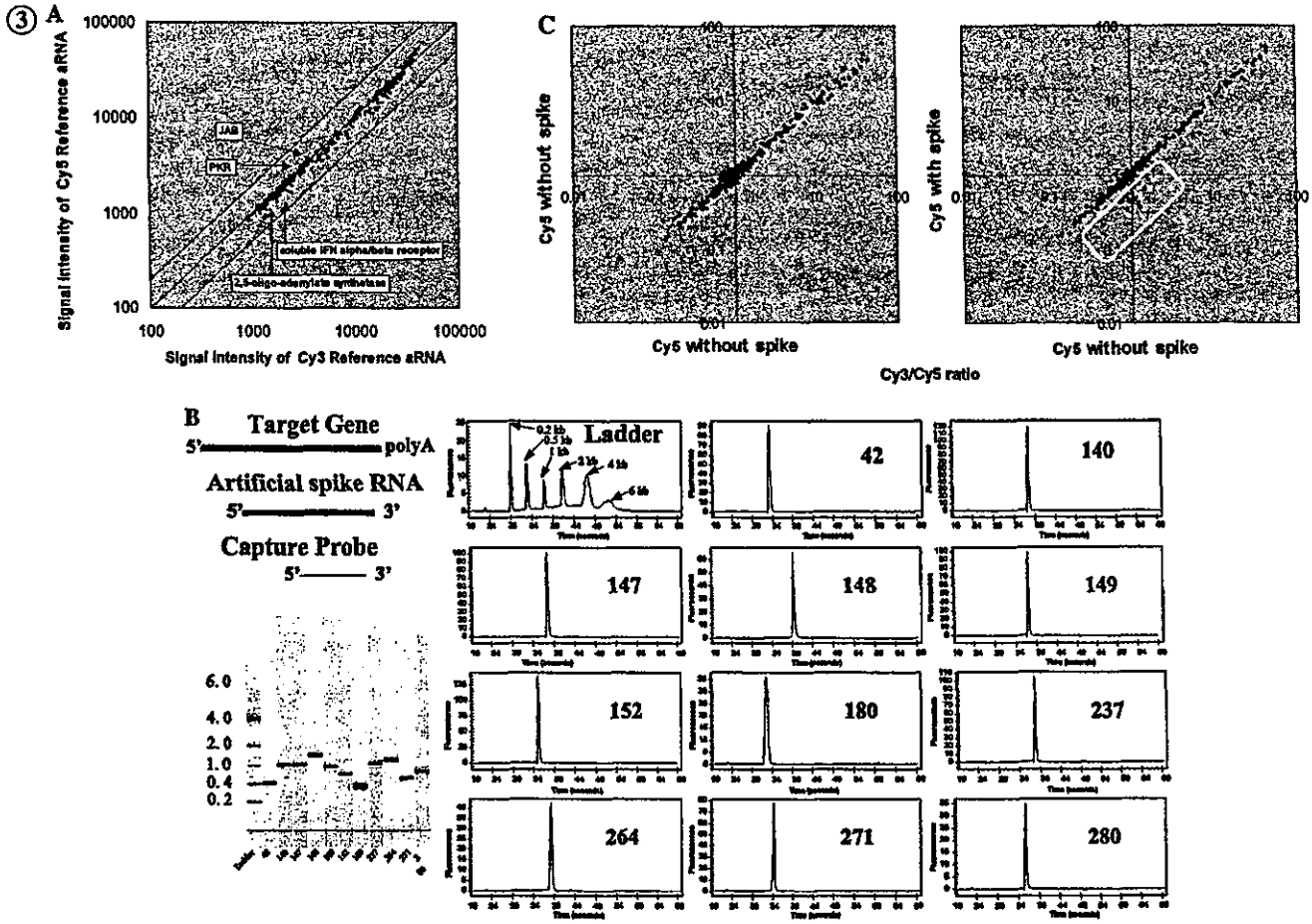
③
A
Signal intensity of Cy5 Reference aRNA
Signal intensity of Cy3 Reference aRNA
JAB
PKR
soluble IFN alpha/beta receptor
2,5-oligo-adenylate synthetase
C
Cy5 without spike
Cy5 with spike
Cy3/Cy5 ratio
B
Target Gene
polyA
Artificial spike RNA
Capture Probe
Ladder
42
140
147
148
149
152
180
237
264
271
280
④
NR
TR
SR
JGS ID
100
258
243
139
142
239
259
249
165
277
174
180
134
111
186
255
99
138
240
232
83
234
246
149
30

Fig. 3. Establishment of the artificial reference RNA. (A) Scatter plot of the mRNA signal level in the four cell RNA mixture. The RNA mixture from four cell lines was covalently modified with Cy3 and Cy5 dyes. The signal levels for typical inflammatory genes, including 2,5-oligoadenylate synthetase (2,5-AS), IFN-α/β receptor, IFN-α receptor, and PKR, are indicated with arrows. (B) Design and purity of the synthetic RNA. The general design of the synthetic RNA (positional relation), including size and position of the probe and the artificial RNA, is shown on the left. Thus, each reference RNA was designed to be longer than the captured probe on the microarray, but not to exceed the size of the target RNA. The purity of the 11 of the synthetic RNA samples is shown. The corresponding gene numbers on our cDNA microarray are shown in each panel and are as follows (GenBank accession number in parentheses): 42, gamma-G globin (X55656); 140, T cell activation antigen (CD27) (M63928); 147, (2′,5′)-oligoadenylate synthetase (D00068); 148, p68 kinase (M35663); 152, CIS3 (AB006967); 180, calcium-binding protein in macrophages (MRP-14), also known as macrophage migration inhibitory factor-related protein (X06233); 237, interleukin 2 receptor β chain (p70-75) (M26062); 264, interferon-induced protein 44 (IFI44) (NM_006417); 271, interleukin 4 (M13982); and 280, hepatocyte growth factor (X16323). (C) Synthetic spiked RNA signal level. The panel on the left represents the scatter plot without any synthetic RNA added to the reference RNA, while the panel on the right shows the reference with added synthetic RNAs. The plot shows the ratio of sample Cy3/Cy5 rather than real signal level. The spots in the white rectangle represent the level of the added synthetic RNAs.

Fig. 4. Hierarchical clustering. cDNA microarray data of 15 patients' samples were analyzed with Genomic Profiler software (MKI, Japan). For clustering, normalization, filtering, and *T* test were essential. Because of interest in predicting clinical outcomes of IFN treatment, we tried to classify the data into two groups, including non-responders (NR) and transient responders (TR)/sustained responders (SR). The accuracy of this prediction was >93%. The corresponding microarray number and according GenBank accession number of the genes responsible for clustering are shown on the right and include: 100, cytoplasmic dynein light chain 1 (U32944); 258, thymosin β-10 (M92383); 243, stathmin (X53305); 139, homeobox 1.4 protein (M74297); 142, cAMP-dependent protein kinase regulatory subunit RI-bet (M65066); 239, alternatively spliced interferon receptor (IFNAR2) (L42243); 259, eukaryotic translation initiation factor 2, subunit 1 α, 35 kDa (BC002513); 249, brain-derived neurotrophic factor precursor (BDNF) (M61176); 165, interleukin 2 (X01586); 277, natural killer cell stimulatory factor (NKSF) (M65290); 174, IFN-responsive transcription factor subunit (M87503); 180, calcium-binding protein in macrophages (MRP-14) also known as macrophage migration inhibitory factor-related protein (X06233); 134, lunatic fringe U94354); 111, protein tyrosine kinase (Syk) (L28824); 186, leukocyte-associated molecule-1 α subunit (LFA-1 α subunit) (Y00796); 255, FLICE-like inhibitory protein short form (U97075); 99, CDK4-inhibitor (p16-INK4) (L27211); 138, α 7B integrin (X74295); 240, interferon-stimulated T-cell α chemoattractant precursor(AF030514); 232, Charcot–Leyden crystal protein (L01664); 83, NADH:ubiquinone oxidoreductase MLRQ subunit (U94586); 234, apoptotic cysteine protease Mch4 (Mch4) (U60519); 246, metallothionein-III (M93311); 149, interferon regulatory factor 1 (X14454); and 30, heat shock 70 kDa protein 1A (BC002453).

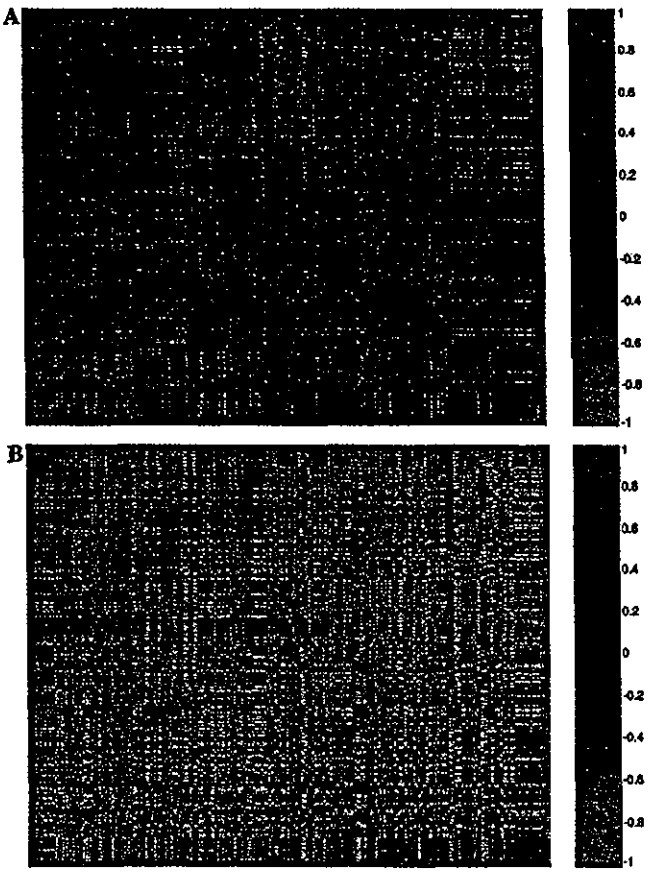

Fig. 5. Typical expression pattern: correlation matrix of 295 gene signals. (A) This expression pattern represented the established standard data as SSDB. Each axis represents genes in consideration. (B) The expression pattern shows an example of NR data as new test sample data. Color and brightness are adjusted according to Eqs. (1)–(3).

Patient No	Prediction	Clinical outcome	sMD (MD/k)*1	
10			6.31	so far from
9			5.97	SSDB center of gravity
8			4.38	
15			3.53	
4			1.96	threshold = 2.0
12			1.90	
13			1.44	
1			1.36	
14			1.09	
6			0.98	
3			0.73	
7			0.67	
11			0.38	
5			0.24	
2			0.24	SSDB center of gravity

Prediction	Clinical Outcome: SR or TR	NR	Total	%
SR or TR	11	0	11	100%
NR	0	4	4	100%
Total	11	4	15	
%	100%	100%		

$P < 0.0005$

Fig. 6. Mahalanobis distance (MD) and classification for efficacy prediction. The resulting MD data were arranged along the scale based on numbers of sMD value. The first column shows the patient number, the second column shows the prediction from our microarray analysis, and the third column shows the actual clinical outcome. Blue represents the NR group, purple represents TR, and red represents the SR group. We have set a threshold at the sMD level of 2.0 to set two groups from the sMD calculation. The hit ratio of prediction to clinical outcome was also shown.

Genomic Profiler software. Because of our interest in predicting IFN efficacy in hepatitis C, we compared the NR group against SR/TR group [33–35]. We chose genes with a 5% discriminated expression pattern (T test) between two groups ([SR vs. NR]∩[(SR + TR) vs. NR]). The hierarchical tree for these genes is shown in Fig. 4. Appropriate groups were assigned to all but one case, a TR case that was classified into the NR group.

Development of a new algorithm for hierarchical clustering

Although the classical method dealing with multi-parameters allowed satisfactory classification of the patients into two groups, this method is not useful for practical purposes. Thus, the entire data set is necessary for interpretation of the results from the classical analysis even for the analysis of a single test sample. In general, clinical diagnosis requires the common scale to compare the analytical data from samples. But a classical classification presents only a relative scale among samples for comparison.

For these reasons, we have developed a new algorithm. This method is based on the calculation of MD. The concept of the MD calculation is outlined in Fig. 1. This is one of the pattern recognition analysis and determines how close or how far from the standard group of interest. Thus, it deals with multi-parameters leading to single parameter, Mahalanobis distance (MD) as a scale, from the center of gravity of SSDB established by a training set shown in Fig. 1. Prior to the MD calculation, it was necessary to establish a SSDB with a training data set randomly selected but with clear and known clinical outcome. The standard expression pattern obtained from the SR/TR group, which was the established data source for SSDB, is shown in Fig. 5A and the new test sample pattern of the NR group is shown in Fig. 5B. The red color represents the higher expression profile and green depicts the lower expression profile with an interrelating style at the same time. Then, the pattern recognition algorithm Eqs. (1)–(3) was applied to compare the two groups. Among these expression patterns, we selected the stably and differentially expressed gene set data. Then, every selected gene expression pattern was correlated to each other like connecting a network. Thus, based on Eqs. (1)–(3), the elements that distinguish the groups shown were selected to create the SSDB. The SSDB was created based on variance and covariance. Once we established the SSDB and the center of gravity of the SSDB, we calculated a MD value for each new test sample (Eq. (4)). We utilized sMD value (divided the MD value by the number of parameters) to reduce MD value (Eq. (5)) and simplify understanding of the results[25]. The classification of IFN efficacy prediction to hepatitis C patients is shown in Fig. 6 and clearly shows that this analysis generates the NR and SR/TR groups and they are predicted with 100% accuracy ($p < 0.005$). The sample size (15 cases) was too small for statistical validation. Further detailed analyses and validation are ongoing in our laboratory and will be reported elsewhere.

Although the MD method is popular in even biological system publications [36,37], an application of MD method to microarray data is not so popular yet. The current studies are not the first published report where MD for analysis of gene expression data [38]. However, that report focused on the differential expression of a causative gene in conjunction with a standard hierarchical clustering algorithm. In our studies, we have attempted to scale the test sample position as a simple understandable parameter with a new pattern recognition algorithm. Once the SSDB scale has been established for a project, the MD can be easily used to classify new data according to the NR and TR/SR groups on an absolute scale (Fig. 6). This system will be acceptable for clinicians as a simple system for understanding the microarray data.

Conclusions

Besides the technical issues, there are many factors that control the variability within a microarray system, including individual differences between patients, the duration of the disease of each patient, different therapeutic protocols, and complications with other diseases. Some of these factors interact with each other, while others are independent. Therefore, an algorithm that allows some variability in the measurements is needed for prediction of therapeutic outcomes. The algorithm presented here appears to satisfy this requirement and it simplifies handling of large data sets. Finally, this algorithm should be generally applicable to the prediction of therapeutic outcome of diseases.

Acknowledgments

We thank Professor Kazunari Akiyoshi and Dr. Akihiko Watanabe (Tokyo Medical and Dental University) for scanning electron microscopy and Professor Kouji Matsushima (University of Tokyo) for helpful discussions.

References

[1] M. Sanchez-Carbayo, Use of high-throughput DNA microarrays to identify biomarkers for bladder cancer, Clin. Chem. 49 (2003) 23–31.
[2] P.F. Macgregor, J.A. Squire, Application of microarrays to the analysis of gene expression in cancer, Clin. Chem. 48 (2002) 1170–1177.
[3] C.H. Chung, P.S. Bernard, C.M. Perou, Molecular portraits and the family tree of cancer, Nat. Genet. 32 (Suppl.) (2002) 533–540.

[4] N.L. Harris, H. Stein, S.E. Coupland, M. Hummel, R.D. Favera, L. Pasqualucci, W.C. Chan, New approaches to lymphoma diagnosis, Hematology (Am Soc Hematol Educ Program) (2001) 194–220.
[5] L.T. Lam, O.K. Pickeral, A.C. Peng, A. Rosenwald, E.M. Hurt, J.M. Giltnane, L.M. Averett, H. Zhao, R.E. Davis, M. Sathyamoorthy, L.M. Wahl, E.D. Harris, J.A. Mikovits, A.P. Monks, M.G. Hollingshead, E.A. Sausville, L.M. Staudt, Genomic-scale measurement of mRNA turnover and the mechanisms of action of the anti-cancer drug flavopiridol, Genome Biol 2 (2001) research0041.
[6] D.G. Beer, S.L. Kardia, C.C. Huang, T.J. Giordano, A.M. Levin, D.E. Misek, L. Lin, G. Chen, T.G. Gharib, D.G. Thomas, M.L. Lizyness, R. Kuick, S. Hayasaka, J.M. Taylor, M.D. Iannettoni, M.B. Orringer, S. Hanash, Gene-expression profiles predict survival of patients with lung adenocarcinoma, Nat. Med. 8 (2002) 816–824.
[7] E. Huang, S.H. Cheng, H. Dressman, J. Pittman, M.H. Tsou, C.F. Horng, A. Bild, E.S. Iversen, M. Liao, C.M. Chen, M. West, J.R. Nevins, A.T. Huang, Gene expression predictors of breast cancer outcomes, Lancet 361 (2003) 1590–1596.
[8] M.L. Lee, F.C. Kuo, G.A. Whitmore, J. Sklar, Importance of replication in microarray gene expression studies: statistical methods and evidence from repetitive cDNA hybridizations, Proc. Natl. Acad. Sci. USA 97 (2000) 9834–9839.
[9] G.C. Tseng, M.K. Oh, L. Rohlin, J.C. Liao, W.H. Wong, Issues in cDNA microarray analysis: quality filtering, channel normalization, models of variations and assessment of gene effects, Nucleic Acids Res. 29 (2001) 2549–2557.
[10] F. Diehl, S. Grahlmann, M. Beier, J.D. Hoheisel, Manufacturing DNA microarrays of high spot homogeneity and reduced background signal, Nucleic Acids Res. 29 (2001) E38.
[11] L. Luo, R.C. Salunga, H. Guo, A. Bittner, K.C. Joy, J.E. Galindo, H. Xiao, K.E. Rogers, J.S. Wan, M.R. Jackson, M.G. Erlander, Gene expression profiles of laser-captured adjacent neuronal subtypes, Nat. Med. 5 (1999) 117–122.
[12] O. Kitahara, Y. Furukawa, T. Tanaka, C. Kihara, K. Ono, R. Yanagawa, M.E. Nita, T. Takagi, Y. Nakamura, T. Tsunoda, Alterations of gene expression during colorectal carcinogenesis revealed by cDNA microarrays after laser-capture microdissection of tumor tissues and normal epithelia, Cancer Res. 61 (2001) 3544–3549.
[13] L. Assersohn, L. Gangi, Y. Zhao, M. Dowsett, R. Simon, T.J. Powles, E.T. Liu, The feasibility of using fine needle aspiration from primary breast cancers for cDNA microarray analyses, Clin. Cancer Res. 8 (2002) 794–801.
[14] D.A. Wigle, I. Jurisica, N. Radulovich, M. Pintilie, J. Rossant, N. Liu, C. Lu, J. Woodgett, I. Seiden, M. Johnston, S. Keshavjee, G. Darling, T. Winton, B.J. Breitkreutz, P. Jorgenson, M. Tyers, F.A. Shepherd, M.S. Tsao, Molecular profiling of non-small cell lung cancer and correlation with disease-free survival, Cancer Res. 62 (2002) 3005–3008.
[15] T.C. Van Der Pouw Kraan, F.A. Van Gaalen, T.W. Huizinga, E. Pieterman, F.C. Breedveld, C.L. Verweij, Discovery of distinctive gene expression profiles in rheumatoid synovium using cDNA microarray technology: evidence for the existence of multiple pathways of tissue destruction and repair, Genes Immun. 4 (2003) 187–196.
[16] T. Yamashita, S. Hashimoto, S. Kaneko, S. Nagai, N. Toyoda, T. Suzuki, K. Kobayashi, K. Matsushima, Comprehensive gene expression profile of a normal human liver, Biochem. Biophys. Res. Commun. 269 (2000) 110–116.
[17] T. Yamashita, S. Kaneko, S. Hashimoto, T. Sato, S. Nagai, N. Toyoda, T. Suzuki, K. Kobayashi, K. Matsushima, Serial analysis of gene expression in chronic hepatitis C and hepatocellular carcinoma, Biochem. Biophys. Res. Commun. 282 (2001) 647–654.
[18] H. Yatsuhashi, K. Yamasaki, T. Aritomi, P. Maria, D. Carmen, O. Inoue, M. Koga, M. Yano, Quantitative analysis of interferon alpha/beta receptor mRNA in the liver of patients with chronic hepatitis C: correlation with serum hepatitis C virus-RNA levels and response to treatment with interferon, J. Gastroenterol. Hepatol. 12 (1997) 460–467.
[19] E. Mizukoshi, S. Kaneko, M. Yanagi, H. Ohno, K. Kaji, S. Terasaki, A. Shimoda, E. Matsushita, K. Kobayashi, Expression of interferon alpha/beta receptor in the liver of chronic hepatitis C patients, J. Med. Virol. 56 (1998) 217–223.
[20] F.L. Dumoulin, U. Wennrich, H.D. Nischalke, L. Leifeld, H.P. Fischer, T. Sauerbruch, U. Spengler, Intrahepatic mRNA levels of interferon gamma and tumor necrosis factor alpha and response to antiviral treatment of chronic hepatitis C, J. Hum. Virol. 4 (2001) 195–199.
[21] H.F. Kawai, S. Kaneko, M. Honda, Y. Shirota, K. Kobayashi, Alpha-fetoprotein-producing hepatoma cell lines share common expression profiles of genes in various categories demonstrated by cDNA microarray analysis, Hepatology 33 (2001) 676–691.
[22] T. Ito, K. Yasui, J. Mukaigawa, A. Katsume, M. Kohara, K. Mitamura, Acquisition of susceptibility to hepatitis C virus replication in HepG2 cells by fusion with primary human hepatocytes: establishment of a quantitative assay for hepatitis C virus infectivity in a cell culture system, Hepatology 34 (2001) 566–572.
[23] A.B. Khodursky, B.J. Peter, N.R. Cozzarelli, D. Botstein, P.O. Brown, C. Yanofsky, DNA microarray analysis of gene expression in response to physiological and genetic changes that affect tryptophan metabolism in *Escherichia coli*, Proc. Natl. Acad. Sci. USA 97 (2000) 12170–12175.
[24] M. Ellis, N. Davis, A. Coop, M. Liu, L. Schumaker, R.Y. Lee, R. Srikanchana, C.G. Russell, B. Singh, W.R. Miller, V. Stearns, M. Pennanen, T. Tsangaris, A. Gallagher, A. Liu, A. Zwart, D.F. Hayes, M.E. Lippman, Y. Wang, R. Clarke, Development and validation of a method for using breast core needle biopsies for gene expression microarray analyses, Clin. Cancer Res. 8 (2002) 1155–1166.
[25] G. Taguchi, J. Rajesh, The Mahalanobis–Taguchi strategy, ed., Wiley, New York, 2002.
[26] J.C. Chang, E.C. Wooten, A. Tsimelzon, S.G. Hilsenbeck, M.C. Gutierrez, R. Elledge, S. Mohsin, C.K. Osborne, G.C. Chamness, D.C. Allred, P. O'Connell, Gene expression profiling for the prediction of therapeutic response to docetaxel in patients with breast cancer, Lancet 362 (2003) 362–369.
[27] C. Workman, L.J. Jensen, H. Jarmer, R. Berka, L. Gautier, H.B. Nielser, H.H. Saxild, C. Nielsen, S. Brunak, S. Knudsen, A new non-linear normalization method for reducing variability in DNA microarray experiments, Genome Biol 3 (2002) research0048.
[28] J.H. Kim, D.M. Shin, Y.S. Lee, Effect of local background intensities in the normalization of cDNA microarray data with a skewed expression profiles, Exp. Mol. Med. 34 (2002) 224–232.
[29] Y.H. Yang, S. Dudoit, P. Luu, D.M. Lin, V. Peng, J. Ngai, T.P. Speed, Normalization for cDNA microarray data: a robust composite method addressing single and multiple slide systematic variation, Nucleic Acids Res. 30 (2002) e15.
[30] X. Wang, S. Ghosh, S.W. Guo, Quantitative quality control in microarray image processing and data acquisition, Nucleic Acids Res. 29 (2001) E75.
[31] E.M. Glare, M. Divjak, M.J. Bailey, E.H. Walters, β-Actin and GAPDH housekeeping gene expression in asthmatic airways is variable and not suitable for normalising mRNA levels, Thorax 57 (2002) 765–770.
[32] P.D. Lee, R. Sladek, C.M. Greenwood, T.J. Hudson, Control genes and variability: absence of ubiquitous reference transcripts in diverse mammalian expression studies, Genome Res. 12 (2002) 292–297.
[33] S. Nishiguchi, T. Kuroki, S. Nakatani, H. Morimoto, T. Takeda, S. Nakajima, S. Shiomi, S. Seki, K. Kobayashi, S. Otani, Randomised trial of effects of interferon-alpha on incidence of

hepatocellular carcinoma in chronic active hepatitis C with cirrhosis, Lancet 346 (1995) 1051–1055.

[34] K. Kuwana, T. Ichida, T. Kamimura, S. Ohkoshi, N. Ogata, T. Harada, K. Endoh, H. Asakura, Risk factors and the effect of interferon therapy in the development of hepatocellular carcinoma: a multivariate analysis in 343 patients, J. Gastroenterol. Hepatol. 12 (1997) 149–155.

[35] M.R. Brunetto, F. Oliveri, M. Koehler, F. Zahm, F. Bonino, Effect of interferon-alpha on progression of cirrhosis to hepatocellular carcinoma: a retrospective cohort study. International Interferon-alpha Hepatocellular Carcinoma Study group, Lancet 351 (1998) 1535–1539.

[36] K.R. Coombes, H.A. Fritsche Jr., C. Clarke, J.N. Chen, K.A. Baggerly, J.S. Morris, L.C. Xiao, M.C. Hung, H.M. Kuerer, Quality control and peak finding for proteomics data collected from nipple aspirate fluid by surface-enhanced laser desorption and ionization, Clin. Chem. 49 (2003) 1615–1623.

[37] O. Samek, H.H. Telle, D.C. Beddows, Laser-induced breakdown spectroscopy: a tool for real-time, in vitro and in vivo identification of carious teeth, BMC Oral Health 1 (2001) 1.

[38] A. Chilingaryan, N. Gevorgyan, A. Vardanyan, D. Jones, A. Szabo, Multivariate approach for selecting sets of differentially expressed genes, Math. Biosci. 176 (2002) 59–69.

THE JOURNAL OF BIOLOGICAL CHEMISTRY
Vol. 279, No. 12, Issue of March 19, pp. 11719–11726, 2004
Printed in U.S.A.

Hepatitis C Virus Core Functions as a Suppressor of Cyclin-dependent Kinase-activating Kinase and Impairs Cell Cycle Progression*

Received for publication, August 4, 2003, and in revised form, December 30, 2003
Published, JBC Papers in Press, January 7, 2004, DOI 10.1074/jbc.M308560200

Kazuyoshi Ohkawa‡, Hisashi Ishida‡, Fumihiko Nakanishi§, Atsushi Hosui§, Keiji Ueda¶, Tetsuo Takehara‡, Masatsugu Hori§, and Norio Hayashi‡‖

From the Departments of ‡Molecular Therapeutics, §Internal Medicine and Therapeutics, and ¶Microbiology, Osaka University Graduate School of Medicine, Suita, Osaka 565-0871, Japan

We investigated how the hepatitis C virus (HCV) core protein affects the cell cycle profile and cell cycle-related molecules by using the HCV core-expressing stable transfectant. Analysis of the cell cycle profile showed that HCV core impaired G_1 to S transition. The E2F-mediated transcription, phosphorylation of the retinoblastoma protein, and cyclin-dependent kinase (CDK) 4 and CDK2 activities were suppressed in HCV core-expressing cells. The expression levels of G_1 phase-related CDKs/cyclins and various CDK inhibitors were not substantially affected by expression of HCV core. When influences of HCV core on CDK-activating kinase (CAK) were examined, the expression levels of the CAK components, CDK7, cyclin H, and MAT1, were not affected. However, formation of the ternary CAK complex, CAK activity, and the CDK2 level with activating phosphorylation were inhibited by expression of the HCV core. The direct effect of HCV core on CAK was further assessed in the cell-free system by adding the *in vitro* translated HCV core protein to the anti-CDK7 immunoprecipitate from the cell. The results showed that HCV core led to dissociation of MAT1 from the CAK complex and suppressed the CAK activity. Furthermore, the binding assay revealed that the HCV core was directed against CDK7. Their interaction occurred mainly in the nucleus by the immunostaining. In conclusion, the HCV core protein interacts with CAK and functions as an extrinsic suppressor of CAK. This may be the molecular basis of HCV core-mediated suppression of cell cycle progression. Our findings suggest a novel mechanism concerning HCV core-mediated alteration in the cell cycle machinery.

Hepatitis C virus (HCV)[1] is a major etiologic cause of acute and chronic hepatitis, liver cirrhosis, and hepatocellular carcinoma (1). HCV is an enveloped virus with a plus-stranded RNA genome of about 9.5 kb in length (2). At least 10 HCV proteins are generated from proteolytic processing of a single large polyprotein precursor in the following order, NH_2-core-envelope 1-envelope 2-p7-nonstructural 2-nonstructural 3-nonstructural 4A-nonstructural 4B-nonstructural 5A-nonstructural 5B-COOH (3, 4). A series of studies have revealed that, among HCV proteins, the HCV core protein substantially affects cellular functions, which may be relevant to the pathogenesis of HCV-related liver diseases. Persistent expression of the HCV core has been reported to lead to malignant transformation of the host cell *in vitro* (5, 6) and *in vivo* (7). HCV core has also been shown to modify the cellular apoptotic cascade under various stimuli (8–11). In addition, the HCV core has been demonstrated to modulate various cellular signal transduction pathways (6, 10, 12–15). Such biological activities of the HCV core to the host cell are thought to be triggered by its direct interaction with cellular proteins. More than 10 HCV core-binding proteins have so far been identified (6, 10, 14–23).

The eukaryotic cell cycle progression is tightly regulated by the cyclin-dependent kinases (CDKs) and cyclins (reviewed in Refs. 24–28). Various CDK-cyclin complexes work in different phases during cell cycle progression; CDK4/6-cyclin D (cycD) plays a major role in the mid-G_1 phase, CDK2-cycE plays a role in the late G_1 phase, CDK2-cycA plays a role in the S phase, and CDC2 (also termed as CDK1)-cycB plays a role in the G_2/M phase. In particular, the retinoblastoma protein pRB is important as a substrate of the CDK-cyclin complexes in the G_1 phase. Once, the complexes of CDK4/6-cycD and CDK2-cycE phosphorylate pRB, the transcription factor E2F is activated. Then the E2F enhances transcription of many genes to enter the S phase. The functions of CDK-cyclin complexes are negatively regulated by CDK inhibitors, which are divided into two groups, a CIP/KIP family ($p21^{CIP1}$, $p27^{KIP1}$, and $p57^{KIP2}$) and an INK4 family ($p16^{INK4A}$, $p15^{INK4B}$, $p18^{INK4C}$, and $p19^{INK4D}$). $p21^{CIP1}$ is an especially well known transcriptional target of the tumor suppressor p53 (29).

The CDK activity is also controlled by both inhibitory and activating phosphorylations (25, 26). The amino-terminal inhibitory phosphorylation sites (Thr-14 and Tyr-15 in human CDK2) are dephosphorylated by CDC25 phosphatases. On the other hand, phosphorylation of a conserved threonine residue in the T-loop (Thr-160 in human CDK2) is required for full activation of CDKs. The CDK-activating kinase (CAK) undergoes the activating phosphorylation of CDKs. CAK is composed of three components, a catalytic subunit CDK7, a regulatory subunit cycH, and an assembly factor MAT1 (30–32). It has been shown that CAK can phosphorylate all cell cycle-related CDKs, CDC2, CDK2, CDK3, CDK4, and CDK6, at least in the cell-free system (30–34).

Thus far, the effects of HCV core on the cell cycle profile and cell cycle-related molecules have been studied by a few investigators (21, 22, 35). It has been reported that the HCV core can

* The costs of publication of this article were defrayed in part by the payment of page charges. This article must therefore be hereby marked "*advertisement*" in accordance with 18 U.S.C. Section 1734 solely to indicate this fact.

‖ To whom correspondence should be addressed: Dept. of Molecular Therapeutics, Osaka University Graduate School of Medicine, 2-2, Yamadaoka, Suita, Osaka 565-0871, Japan. Tel.: 81-6-6879-3440; Fax: 81-6-6879-3449; E-mail: hayashin@moltx.med.osaka-u.ac.jp.

[1] The abbreviations used are: HCV, hepatitis C virus; CDK, cyclin-dependent kinase; cycD, cyclin D; CAK, CDK-activating kinase; aa, amino acids; GST, glutathione *S*-transferase; CTD, carboxyl-terminal domain; CL2, BNL CL.2; IP, immunoprecipitation; MOPS, 4-morpholinepropanesulfonic acid.

bind to both p53 and $p21^{CIP1}$ and that its binding to p53 up-regulates the p53-dependent transcription activity of $p21^{CIP1}$ in cultured cells transiently transfected with HCV core-expressing plasmid (21, 22). The stable transfectant with HCV core-expressing plasmid derived from Chinese hamster ovary cells has also been shown to impair the cell cycle regulation accompanied by enhancement of $p21^{CIP1}$ expression (35). However, molecular mechanisms concerning HCV core-mediated modulation on the cell cycle-related molecules other than the $p53/p21^{CIP1}$ system have not been elucidated. To solve this, we investigated the effects on cell cycle-related molecules caused by persistent expression of the HCV core in cultured murine normal liver cells. In this process, we found that CAK is a novel target of the HCV core and that the HCV core suppresses cell cycle progression by a direct inhibitory effect on CAK assembly and activity.

EXPERIMENTAL PROCEDURES

Plasmid Constructs—The HCV core-expressing plasmid pc/3EFΔNCTH, which was constructed from a mammalian expression vector pc/3EFpro, carried the whole HCV core gene and the 5'-part of the envelope 1 gene of a genotype 1b HCV strain (36). Both pc/3EFpro and pc/3EFΔNCTH were kindly provided by Dr. T. Wakita (Department of Microbiology, Tokyo Metropolitan Institute of Medical Science). pF/core(1–191) was synthesized from pCMVtag2B (Stratagene) by inserting the HCV core gene (amino acids (aa) 1–191) downstream of the T3 promoter and used for the *in vitro* translation. pTALluc (Clontech) encoded the luciferase gene driven by the minimal TAL promoter. pE2Fluc (Clontech) was a derivative of pTALluc and possessed a repeated sequence of the E2F-responsive element upstream of the TAL promoter. pCMVβ (Clontech) expressed the β-galactosidase gene driven by the cytomegalovirus promoter. Plasmids p5GEX/hCDK2, p5GEX/hCDK7, p5GEX/hcycH, and p5GEX/hpRB(379–793) were used for the production of human CDK2, CDK7, cycH, and pRB as glutathione *S*-transferase (GST) fusion proteins. To construct these plasmids, whole coding regions of the cDNAs for CDK2, CDK7, and cycH and the part of the pRB cDNA (corresponding to aa 379–793 of pRB) were obtained by PCR using a cDNA sample from human hepatoma-derived cell lines, Huh-7 (37) (for CDK2) and HepG2 (38) (for pRB), or using the human adult liver cDNA library (Clontech) (for CDK7 and cycH). The cDNA fragments were cloned into the multicloning site of the plasmid p5GEX-1 (Amersham Biosciences). Plasmid p5GEX/core(1–122) expressed the fusion protein of GST with the truncated HCV core protein (aa 1–122). Plasmid pGCTD produced the carboxyl-terminal domain (CTD) of the largest subunit of RNA polymerase II fused to GST (39), which was a kind gift from Dr. William S. Dynan (Institute of Molecular Medicine and Genetics, Medical College of Georgia).

Cell Culture and Protein Extraction—A murine normal liver cell line, BNL CL.2 (CL2) (40), and a human hepatoma cell line, HepG2 (38), were grown in Dulbecco's modified Eagle's medium supplemented with 10% fetal calf serum, 100 μg/ml of streptomycin sulfate, 100 units/ml of penicillin G sodium, and 0.25 μg/ml of amphotericin B at 37 °C in a 5% CO_2. Three independent clones of the HCV core-expressing cells (designated as CL2 core-I, -II, and -III) and the negative control cells (mock) were established from the CL2 cells as described elsewhere (15, 41). The total cellular protein was extracted with the lysis buffer containing 50 mM Tris-HCl (pH 7.5), 2 mM EDTA, 2 mM EGTA, 50 mM NaF, 5 mM $Na_4P_2O_7$, 0.1% 2-mercaptoethanol, 1% Triton X-100, 10 mM β-glycerophosphate, 0.5 mM sodium vanadate, 1 μg/ml aprotinin, 1 μg/ml leupeptin, 1 μg/ml pepstatin, and 1 mM phenylmethylsulfonyl fluoride and used for Western blotting, immunoprecipitation (IP), kinase assay, and *in vitro* binding assay. The nuclear fraction was obtained from the cells by the method described elsewhere (42).

Analyses of Cell Growth—To examine the cell growth curve, 5×10^3 of CL2 mock and core cells were seeded on a 96-well culture plate. After 24, 48, 72, and 96 h, the net number of viable cells were assessed colorimetrically using the water-soluble tetrazolium (2-[2-methoxy-4-nitrophenyl]-3-[4-nitrophenyl]-5-[2,4-disulfophenyl]-2*H*-tetrazolium monosodium salt) (Roche Applied Science) (43). This assay is based on the cleavage of the tetrazolium salt by mitochondrial dehydrogenase in viable cells. For the assay, 10 μl of the water-soluble tetrazolium reagent was added to the 100-μl culture medium, followed by the incubation at 37 °C for 1 h. Then the optical density at 450 nm was measured. The assay was done in quadruplicate, and the values were expressed as the means ± S.D.

Analysis of Cell Cycle Profile—The flow cytometric analysis to examine the cell cycle profile was done by the method described previously (44) with minor modifications. Briefly, the CL2 mock and core cells were fixed with 70% ethanol and stored at −20 °C. After centrifugation, the pellet was resuspended in the phosphate-buffered saline and incubated for 30 min in the presence of 0.2 mg/ml of propidium iodine and 1 mg/ml RNase A to stain the cellular double-stranded nucleic acid. After filtration with a 60-μm mesh filter, the cell suspension was analyzed on a FACScaliber flow cytometer and with Cellquest software (Becton Dickinson). Percentages of cells representing G_0/G_1, S, and G_2/M phases were determined.

Reporter Gene Assay—For cotransfection analysis, 8.0×10^4 of CL2 cells were seeded in a 35-mm-diameter culture dish and cotransfected of 0.5 μg of the reporter plasmid (pE2Fluc or pTALluc) with 0.5 μg of the effector plasmid (pc/3EFpro or p/3EFΔNCTH) using 6 μg of the cationic liposome (Lipofectin; Invitrogen). For the assay using cells constitutively expressing the HCV core, 8.0×10^4 of CL2 mock or 1.2×10^5 of CL2 core cells were seeded and transfected with 1 μg of the reporter plasmid (pE2Fluc and pTALluc). In all of the reporter gene assays, 0.1 μg of pCMVβ was also transfected. Two days after transfection, the cells were lysed and subjected to the luciferase and β-galactosidase assays. The luciferase activity was normalized for transfection efficiency based on the result of β-galactosidase assay. To determine the E2F-mediated transcription activity, the ratio of the fold activity in transfection with the pE2Fluc to that in transfection with pTALluc was calculated. All of the assays were done in quadruplicate, and the values were expressed as the means ± S.D.

Northern Blot Analysis—For Northern blot analysis, total cellular RNA was extracted from CL2 mock and core cells using a TRIZOL reagent (Invitrogen) based on the guanidine-isothiocyanate method. The poly(A)$^+$ RNA was selected from 50 μg of the total cellular RNA with an oligo(dT) column (Roche Applied Science). The sample was electrophoresed, transferred to a nylon membrane (Hybond N; Amersham Biosciences), and hybridized to the cDNA probe. After washing, the membrane was autoradiographed. The membrane was dehybridized by boiling in 0.5% SDS and further used for the hybridization to detect β-actin mRNA as a loading control (data not shown).

Antibodies—An antibody to pRB was obtained from Pharmingen. Antibodies to CDK4, CDK6, cycD1, CDK2, cycE, cycA, CDC2, cycB1, p53, $p21^{CIP1}$, $p27^{KIP1}$, CDK7, cycH, and MAT1 were purchased from Santa Cruz. An antibody to phosphorylated CDK2 at the Thr-160 residue (pT^{160}-CDK2) came from Cell Signaling. An antibody to GST was from Amersham Biosciences. A mouse monoclonal antibody to HCV core (45) was kindly provided by Dr. T. Wakita (Department of Microbiology, Tokyo Metropolitan Institute of Medical Science).

Immunofluorescence Staining and Confocal Microscopy—The CL2 core-I cells were plated on a two-well chamber slide. One day after seeding, the cells were fixed with 3% paraformaldehyde, 2% sucrose in phosphate-buffered saline for 30 min and permeabilized with ice-cold methanol for 3 min. After the blocking reaction with 10% fetal calf serum for 30 min at room temperature, the cells were incubated at 4 °C for 14 h with two primary antibodies, a mouse monoclonal HCV core antibody, and a rabbit polyclonal CDK7 antibody. Bound primary antibodies were revealed by incubation for 30 min at room temperature with Alexa Fluor 488-conjugated anti-mouse IgG (Molecular Probes) and Cy3-conjugated anti-rabbit IgG (Jackson Immunoresearch). Finally, a coverslip was mounted in the mounting medium (Vectashield; Vector Laboratories) with 4',6-diamidino-2'-phenylindole-dihydrochroride, and the cells were examined by the confocal microscopic analysis using a Radiance 2100 BLD system (Bio-Rad). Colocalization of green and red signals in a single pixel produces yellow, whereas separated signals remain green or red.

Western Blot Analysis and Immunoprecipitation—For Western blot analysis, the total cellular protein was fractionated by SDS-polyacrylamide gel electrophoresis and blotted onto a membrane. After blocking with milk, the membrane was incubated with the specific antibody, followed by further incubation with a secondary antibody. Finally, the immune complex was detected by an enhanced chemiluminescent assay (Super Signal; Pierce). As for the IP reaction, 250–500 μg of the total cellular protein was precleared with protein A-Sepharose beads (Amersham Biosciences) at 4 °C for 1 h. After centrifugation, the supernatant was incubated with the specific antibody at 4 °C for 1–2 h. Then the beads was added, and the sample was further incubated at 4 °C for 1 h. After the extensive washing, the product was used for Western blot analysis and the kinase assay. In some experiments, the binding reaction of the IP product with the *in vitro* translation product was carried out at 4 °C for 3 h, prior to the subsequent experiments. The *in vitro*